
GEOSPATIAL FOUNDATION MODELS TO ENABLE PROGRESS ON SUSTAINABLE DEVELOPMENT GOALS

A PREPRINT

Pedram Ghamisi¹, Weikang Yu¹, Xiaokang Zhang², Aldino Rizaldy¹, Jian Wang³, Chufeng Zhou³,
Richard Gloaguen¹, Gustau Camps-Valls⁴

¹Helmholtz-Zentrum Dresden-Rossendorf (HZDR), 09599 Freiberg, Germany

²Wuhan University, 430072 Wuhan, China

³Wuhan University of Science and Technology, 430081 Wuhan, China

⁴Universitat de València, 46010 València, Spain

ABSTRACT

Foundation Models (FMs) are large-scale, pre-trained artificial intelligence (AI) systems that have revolutionized natural language processing and computer vision, and are now advancing geospatial analysis and Earth Observation (EO). They promise improved generalization across tasks, scalability, and efficient adaptation with minimal labeled data. However, despite the rapid proliferation of geospatial FMs, their real-world utility and alignment with global sustainability goals remain under-explored. We introduce SustainFM, a comprehensive benchmarking framework grounded in the 17 Sustainable Development Goals with extremely diverse tasks ranging from asset wealth prediction to environmental hazard detection. This study provides a rigorous, interdisciplinary assessment of geospatial FMs and offers critical insights into their role in attaining sustainability goals. Our findings show: (1) While not universally superior, FMs often outperform traditional approaches across diverse tasks and datasets. (2) Evaluating FMs should go beyond accuracy to include transferability, generalization, and energy efficiency as key criteria for their responsible use. (3) FMs enable scalable, SDG-grounded solutions, offering broad utility for tackling complex sustainability challenges. Critically, we advocate for a paradigm shift from model-centric development to impact-driven deployment, and emphasize metrics such as energy efficiency, robustness to domain shifts, and ethical considerations.

Keywords Foundation Models, Earth Observation, Sustainable Development Goals, Geospatial AI, Benchmarking.

1 Introduction

The convergence of artificial intelligence (AI) and Earth observation (EO) technologies has launched an unprecedented era of capabilities for addressing global sustainability challenges [1]. The Sustainable Development Goals (SDGs), established by the United Nations General Assembly in 2015, represent a comprehensive framework for addressing global challenges through 17 interconnected goals spanning social, economic, and environmental dimensions [2, 3, 4]. These goals aim to achieve a better and more sustainable future by 2030, addressing critical issues including poverty, inequality, climate change, environmental degradation, peace, and justice [5, 6, 7]. EO techniques significantly contribute to sustainable development by providing critical data and insights that support the achievement of SDGs [6, 7, 8]. From monitoring climate change, biodiversity, and water resources to enhancing food security, urban planning, and disaster resilience [9, 10, 11, 12], EO provides critical information for tracking environmental and socio-economic trends. Through supporting evidence-based policy and providing an enormous amount of up-to-date data, EO accelerates progress toward a more sustainable, equitable, and resilient future [13, 14].

The scale and complexity of EO data necessitate automated analytical tools capable of handling diverse, multimodal spatio-temporal datasets [15]. Foundation models (FMs) have emerged as a transformative solution, offering un-

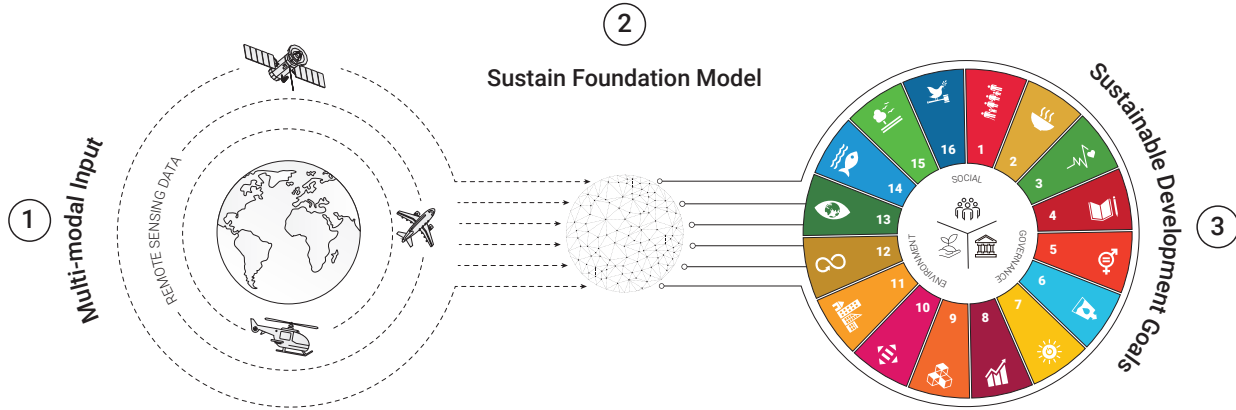


Figure 1: Summary of the SustainFM benchmark. By bringing together domain experts and AI specialists (SDG 17: Partnerships for the Goals), and providing a collection of 16 datasets aligned with the first 16 SDGs, from six continents, spatial resolutions ranging from 0.5 m to 30 m, and multiple tasks grounded in real-world applications, SustainFM aims to provide a testbed to analyze the applicability and real impact of foundation models.

precedented capabilities for geospatial applications through their ability to process vast amounts of heterogeneous data and generalize across multiple downstream tasks [16, 17]. FMs represent a paradigm shift in AI, characterized by large-scale pre-training on extensive, diverse datasets using self-supervised [18] or fully supervised learning approaches [19]. These models normally contain billions of parameters (e.g., Google’s SegGPT [20] with over 3 billion and Meta’s DINOv2 [21] with around 1 billion parameters), and leverage vast computational resources to learn detailed patterns and representations from massive datasets, which enables them to generalize across a wide range of downstream tasks. With this definition, they serve as a universal backbone to support a wide range of applications across domains such as natural language processing (NLP), computer vision, and (geo)scientific computing. The term foundation emphasizes its role in providing a pre-trained, transferable representation that can be fine-tuned or adapted for domain-specific applications. Specifically, geospatial FMs are pre-trained on vast amounts of airborne and space-borne data and can then be adapted for downstream EO tasks, such as land cover classification, change detection, or disaster response mapping, without requiring separate models to be trained from scratch for each task [22]. Key characteristics of FMs include: (1) **Scalability** through efficient, distributed training; (2) **Generalization** via transferable representations across tasks; and (3) **Few-/Zero-shot Learning**, enabling adaptation with little or no labeled data.

The evolution of geospatial FMs has witnessed explosive growth, progressing from single-modal approaches focusing on optical satellite imagery [23, 24, 25] to sophisticated multi-modal architectures that integrate diverse data sources [26, 27, 28, 29], including optical, SAR, hyperspectral, and auxiliary geospatial information [30, 31]. However, the rapid growth in the number of FMs over such a short period has led to a saturation of new architectures, resembling the clear trajectory we witnessed in the EO community during the deep learning boom around 2016, often marked by incremental improvements and limited consideration of their societal, environmental, and economical impact. A fundamental gap remains in grounding model development with global sustainability objectives. To see the actual impact of FMs on real-world challenges, such as climate monitoring, resource management, and humanitarian applications, there needs to be a stronger focus on the deployment phase (downstream tasks), which is widely regarded as the ultimate goal of Responsible AI in EO [32].

On the other hand, current evaluation approaches primarily focus on task-specific accuracy metrics [33, 34, 35], providing limited insight into the model’s utility for addressing complex sustainability challenges. This gap is particularly concerning when FMs are increasingly applied in domains directly related to human welfare, environmental conservation, and economic development areas, where decisions carry profound consequences beyond accuracy scores. To truly unlock their potential, FMs should be assessed not only on technical sophistication but also on their contributions to social equity, environmental protection, and economic sustainability. Yet, such dimensions are often absent in current evaluation frameworks, underscoring the urgent need for a systematic benchmark that integrates mainstream FMs with multi-source datasets aligned to the SDGs.

To address this, we must shift the emphasis from mere model development to the deployment phase [36], where FMs are evaluated based on their impact on complex socio-environmental contexts. Performance evaluation should go beyond traditional benchmarks and include real-world scenarios, social good, and ethical considerations in the deployment stage. Furthermore, the interdisciplinary views of both AI and domain experts are required to ensure that

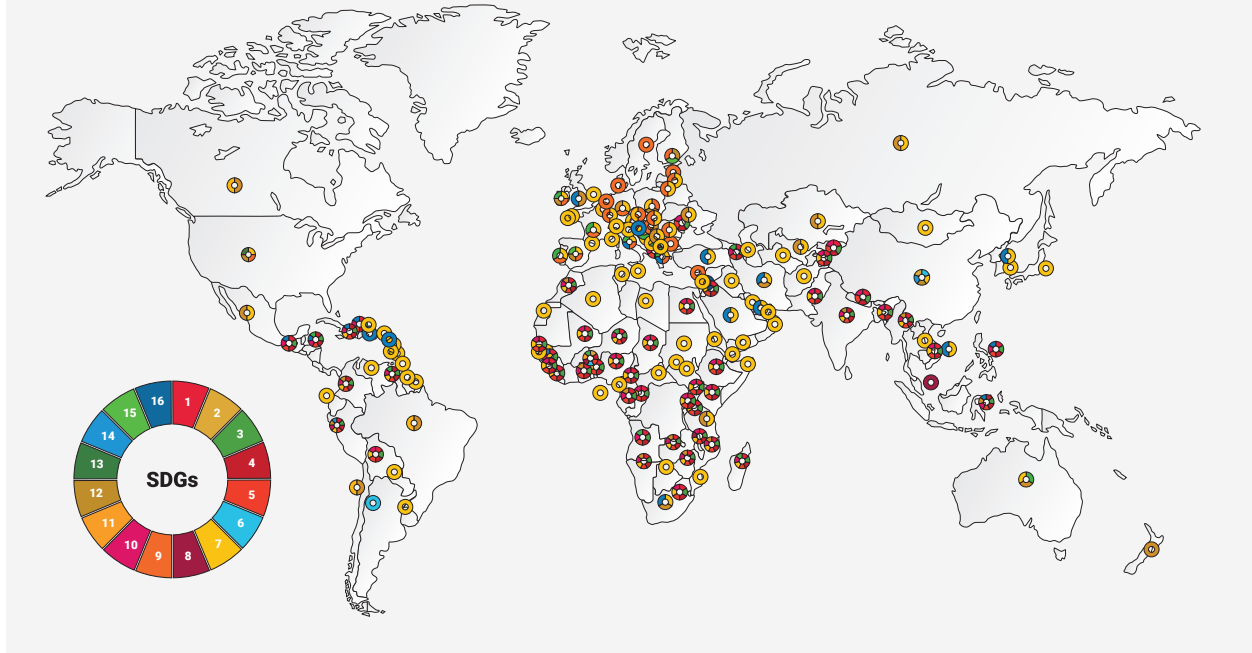


Figure 2: Geographic coverage of the SustainFM benchmark, which spans over 200 regions across 6 continents to support a wide range of EO tasks aligned with the SDGs.

FMs are not only optimized for accuracy but also for their contribution to long-term societal benefits [37]. Without this shift, we risk an unsustainable model development cycle with no real-world impacts.

In this paper, we move beyond the current hype of FMs to adopt an evidence-based approach to answer this question:

1. *Do we need FMs, or are traditional, purpose-specific deep learning models sufficient for EO tasks?*
2. *What evaluation criteria best capture the effectiveness and responsibility of FMs in EO, beyond task-specific accuracy?*
3. *Can FMs be systematically leveraged to support scalable, SDG-grounded solutions for geospatial challenges?*

Through systematic evaluation across key criteria, including accuracy, transferability, data efficiency, energy costs, and operational impact, we aim to provide a grounded, rigorous assessment that challenges assumptions and clarifies the actual added value, if any, of FMs in this domain. Ultimately, our goal is to contribute to global sustainability objectives and promote social good, a key aspect that has been undermined in many current geospatial FMs. To evaluate FMs in EO rigorously, we introduce SustainFM, a benchmark aligned with all 17 SDGs that provides new EO datasets, leverages pretrained FMs, and evaluates them for global sustainability, as conveyed in Fig. 1.

This paper makes four key contributions. Scientifically, it introduces SustainFM, the first comprehensive benchmarking framework for evaluating FMs against the SDGs, setting new standards for responsible AI in Earth observation. Methodologically, it advances beyond accuracy-focused assessments by integrating critical metrics such as energy efficiency, transferability, and environmental impact, promoting a paradigm shift from performance-driven development to impact-driven deployment. Societally, it demonstrates how FMs can enable scalable solutions to global challenges while ensuring equitable outcomes across diverse communities. Environmentally, it quantifies the carbon footprint of model training and advocates for energy-efficient strategies that reduce emissions without sacrificing performance. By aligning geospatial AI with the SDG framework, this work lays a crucial foundation for leveraging advanced AI responsibly to address pressing sustainability challenges.

Table 1: Description of the SustainFM Benchmark, including SDG-related tasks (applications) with sensor type, resolution, scale, AI task, patch size, and number of patches.

#SDG	Application	Sensor	Resolution	Scale	AI Task	Patch Size	#Patches
1	Asset Wealth Index Regression	Landsat+VIIRS	30m	Africa	Reg.	256 × 256	86,936
2	Cropland Change Detection	Gaofen-2	0.5-2m	China	CD	256 × 256	2,400
3	Children’s Health Regression	Landsat+VIIRS	30m	Africa	Reg.	256 × 256	105,582
4	Women Educational Attainment Regression	Landsat+VIIRS	30m	Africa	Reg.	256 × 256	117,062
5	Women Health Regression	Landsat+VIIRS	30m	Africa	Reg.	256 × 256	94,866
6	Urban BOW Detection	Gaofen-2	1m	China	Seg.	256 × 256	1,645
7	Solar Farm Identification	Sent-2	10m	Global	Seg.	256 × 256	10,230
8	Detection of Settlements without Electricity	Sent-1+Sent-2+Landsat+VIIRS	10m	Malawi	Seg.	800 × 800	98
9	Industrial Smoke Plume Detection	Sent-2	10m	EU	Seg.	120 × 120	25,100
10	Sanitation Index Regression	Landsat+VIIRS	30m	Africa	Reg.	256 × 256	89,271
11	Urban Building Change Detection	Google Earth	0.5m	U.S.	CD	1024 × 1024	637
12	Mining Change Detection	Google Earth	1.2m	Global	CD	256 × 256	71,711
13	Wildfire Burn Scar Detection	HLS	30m	U.S.	Seg.	512 × 512	1,068
14	Marine Pollution Detection	Sent-2	10m	Global	Seg.	240 × 240	2,803
15	Flood Mapping	Sent-1+Sent-2	10m	Global	Seg.	256 × 256	1,688
16	War-induced Damage Classification	Planet Scope	3m	Regional	Cls.	128 × 128	13,460

2 SustainFM

Achieving the SDGs requires reliable tools to monitor progress across complex, interconnected systems. Despite the global availability of satellite data, assessing the real-world impact of development processes and their alignment with sustainability goals remains a major challenge [7]. To address this gap, we introduce SustainFM, a benchmark dataset for monitoring 16 SDGs using EO data. Specifically, SustainFM spans over 200 countries and regions across continents (Fig. 2), covering diverse sensor types and spatial resolutions (0.5 m–30 m), including Landsat, Sentinel-1/2, VIIRS, Gaofen-2, HLS, Google Earth, and PlanetScope, to reflect the complexity of global sustainability challenges. It integrates 16 real-world tasks aligned with the first 16 SDGs, including asset wealth prediction, health estimation, solar farm and settlement mapping, as well as detection of industrial smoke, marine pollution, and conflict-related damage. These tasks represent key learning paradigms, including regression (Reg.), classification (Cls.), semantic segmentation (Seg.), and change detection (CD). Through collaboration with experts from diverse fields, including remote sensing, machine learning, statistics, and AI ethics, SustainFM also contributes to SDG-17 (Partnerships for the Goals), bridging the gap between academic benchmarks and real-world impact. Table 1 summarizes the EO datasets in SustainFM, with each entry corresponding to a task linked to a specific SDG application. Designed as a testbed for downstream tasks, SustainFM supports systematic evaluation of FM performance, generalization, and energy efficiency across data modalities and learning settings. Below, we introduce the 16 building blocks of SustainFM, each aligned with a specific SDG, along with the corresponding evaluation protocols.

2.1 No Poverty (SDG-1)

Eradicating poverty in all its forms is a central objective of sustainable development. Effective monitoring of poverty requires capturing spatial and socioeconomic disparities, which can be challenging using traditional survey methods alone. EO data offers a complementary approach by providing large-scale insights into analyzing poverty triggers from a bird’s-eye view of residential conditions, including human settlements, infrastructure quality, and resource distribution [38, 39, 40]. However, human development circumstances within society, such as human well-being, education, and gender equality, still face difficulties in being directly measured or indicated by EO data due to the lack of labels.

To tackle these challenges, recent literature has seen innovations that indicate the development of such themes by using human survey data and subsequently connecting these survey data with satellite images via regression tasks [41, 42]. One possible solution is to use the Demographic and Health Surveys (DHS) survey data, which has been widely explored for its relationship with the satellite images. For example, SustainBench [43] explored six variables in the DHS dataset, including asset wealth index, women’s BMI, child mortality rate, women’s educational attainment, water quality index, and sanitation index. In particular, the SustainBench processes the DHS survey data by converging the localized entries into cluster-level data, and subsequently collects satellite images that are geographically centered around each surveyed cluster’s geocoordinates. These satellite images comprise both daytime images from the Landsat 5, 7, and 8 satellites and nightlight images from the DMSP and VIIRS satellites.

Therefore, SustainFM includes an asset wealth index regression task to assess localised poverty using the DHS data from SustainBench [43]. Wealth is estimated at the cluster level using a principal component analysis (PCA) of household assets, yielding a scalar index averaged across surveyed households in each cluster. The dataset comprises

2,079,036 households across 86,936 clusters in 48 countries, based on DHS surveys conducted between 1996 and 2019.

2.2 Zero Hunger (SDG-2)

Ensuring food security and promoting sustainable agriculture is critical to combating hunger and malnutrition. Agricultural productivity is influenced by factors such as weather conditions, soil health, and water availability, all of which can be monitored using EO data. Satellite imagery enables large-scale assessment of cropland distribution, yield estimation, and the impact of natural disaster incidents [44, 45]. Within these perspectives, monitoring the fast and dynamic changes in cropland is a vital task to address food safety problems that are essential to zero hunger [46], which can provide timely cropland information to ensure cropland production and food security [47].

SustainFM incorporates the Cropland Change Detection (CLCD) dataset to support food security and sustainable agricultural land management [48], as shown in Fig. 3. It comprises 600 cropland change samples derived from the Gaofen-2 satellite in Guangdong Province, China, in 2017 and 2019. Each group of samples consists of two images of 512×512 pixels and a corresponding binary label indicating the cropland change. Each pair is annotated with binary labels indicating cropland conversion, including changes to buildings, roads, lakes, and bare soil, which are the key factors that threaten agricultural sustainability.

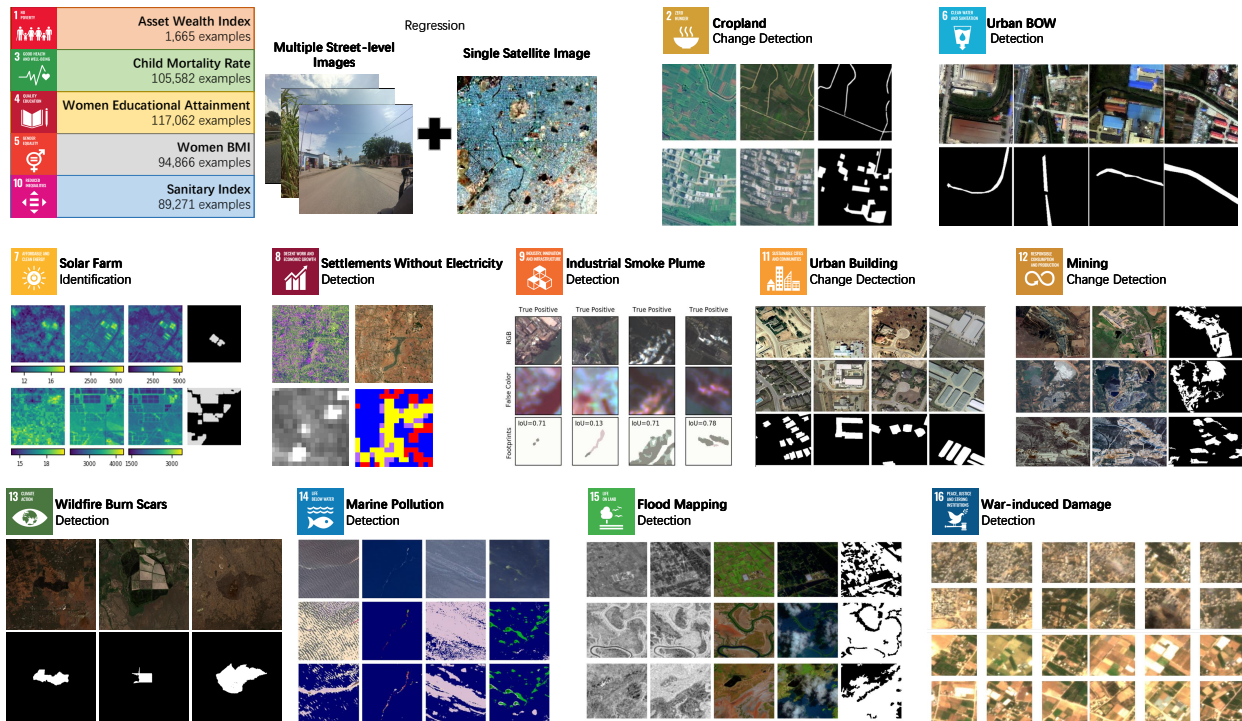


Figure 3: SDGs tasks and data samples in the SustainFM benchmark.

2.3 Good Health and Wellbeing (SDG-3)

Improving health outcomes and ensuring access to healthcare services are vital for enhancing global well-being. Health outcomes are shaped by a complex interplay of environmental and infrastructural factors, including air quality, climate, land use, and access to clean water and healthcare services. EO data offer spatially explicit indicators that can support public health interventions by identifying at-risk populations and monitoring environmental stressors associated with disease and mortality [49, 50, 51].

The SustainFM involves a task of children’s health regression based on the DHS survey dataset of SustainBench [43]. Specifically, the children’s health is indicated by the cluster-level child mortality rate that covers children who were age 5 or younger at the time of the DHS survey or who had died (age 5 or younger) no earlier than the year prior to the DHS survey. After identifying the qualifying children, the child mortality rate is further calculated as the number of

deaths per 1,000 children within each cluster. This dataset consists of 105,582 cluster-level labels for child mortality rates computed from 1,936,904 children under age 5.

2.4 Quality Education (SDG-4)

Access to quality education is essential for promoting equitable development and reducing social inequalities. Educational access is often influenced by geographical factors, including the proximity of schools, transportation networks, and infrastructure quality. Although EO data cannot directly measure educational outcomes, the triggers for quality education, such as school locations, population density, and education accessibility, are observable on satellite images [52, 53]. This information helps identify educational disparities, especially in rural and marginalized areas.

Therefore, SustainFM includes an analysis of women’s educational attainment, based on the DHS survey dataset from SustainBench [43]. The educational attainment metric is derived by calculating the cluster-level mean of education years for women aged 15-49. To mitigate outliers, education years are capped at 18, a common threshold in surveys. Finally, the dataset includes 122,435 cluster-level labels, computed from data on 3,013,286 women across 56 countries.

2.5 Gender Equality (SDG-5)

Achieving gender equality requires eliminating discrimination and ensuring equal access to resources, services, and opportunities. EO-derived indicators such as vegetation cover, urbanization levels, and environmental quality can provide valuable perspectives into the underlying social, economic, and environmental conditions that influence women’s health [41]. By linking these spatial features to BMI outcomes, researchers and policymakers can identify regions where women are particularly vulnerable to malnutrition or obesity due to systemic inequality. This enables the development of geographically targeted, evidence-based interventions aimed at improving women’s health and well-being, thereby addressing one of the critical dimensions of gender inequality.

The SustainFM involves a task of women’s BMI index regression from satellite images based on the DHS dataset of SustainBench [43]. Predicting the BMI from the EO data has demonstrated effectiveness in several previous studies [54, 55], while the dataset from SustainBench solely focuses on the BMI indexes surveyed from women. In particular, this dataset contains 94,866 cluster-level BMI labels computed from 1,781,403 women of childbearing age (15-49), excluding pregnant women.

2.6 Clean Water (SDG-6)

Ensuring universal access to clean water and sanitation is vital for public health and sustainable development. Water scarcity, pollution, and uneven distribution of freshwater resources pose major challenges [56]. EO data plays a key role in monitoring surface water extent and quality [57, 58]. In the residential area, the black and odorous water (BOW) seriously affects the ecological balance of rivers and the health of people living nearby. Therefore, detecting the appearance of such water with EO data helps the authorities with water environment treatment that can improve the water quality in accurate, localized areas.

SustainFM includes an urban black and odorous water (BOW) detection task using the RSBD dataset [59], which comprises 329 multispectral images from the Gaofen-2 satellite in Yantai, China, as shown in Fig. 3. The RSBD dataset is constructed in Yantai, a major port city in the Bohai Sea region in China, which is bordered by the Yellow Sea to the south and the Bohai Sea to the north. Since the northern coastal areas of China have experienced increasing water and energy shortages, as well as offshore environmental pollution, the BOW in the urban area has become a major obstacle to the development of Yantai City, which has limited the sustainable development of the regional economy and society. Moreover, pixel-level annotations of BOW enable the training of segmentation models to detect contaminated water, thereby supporting water quality management in urban settings.

2.7 Affordable and Clean Energy (SDG-7)

Reliable access to clean energy is critical for sustainable development and climate mitigation. With renewables surpassing fossil fuels in several countries (e.g., Germany, for instance, reached a 52% renewable share in 2024 [60]), tracking the deployment of clean energy infrastructure is increasingly important. EO data enables large-scale identification and monitoring of energy assets, such as solar farms, informing the global transition to low-carbon systems [61, 62, 63].

SustainFM includes a solar farm identification task based on the GloSoFarID dataset [64], which provides 13,703 multispectral Sentinel-2 image samples with pixel-level annotations. The dataset includes global solar farm samples

from 2017 to 2018 and U.S. samples from 2022 to 2023, covering installations at a 10m spatial resolution (shown in Fig. 3). These EO-derived maps support the analysis of solar infrastructure expansion and guide decision-making in clean energy planning.

2.8 Decent Work and Economic Growth (SDG-8)

Promoting sustained economic growth and ensuring decent work opportunities are central to reducing poverty and inequalities. Economic development can be indicated by many factors such as urbanization, transportation networks, and infrastructural construction. In modern society, these indicators are significantly influenced by the electricity supply, which is fundamental to everyday life and industrial production [65]. However, some regions, especially in less developed countries, still lack an electricity supply, which not only significantly limits economic development but also affects the living quality of local residents [66, 67].

The SustainFM involves the task of detecting the settlements without electricity based on the detection of settlements without electricity (DSE) dataset [68]. This dataset was released as part of the 2021 data fusion contest organized by the IEEE Geoscience and Remote Sensing Society (GRSS). The dataset is derived from the Dezda and Salima sectors in Malawi, comprising 98 tiles of multimodal EO data collected from Sentinel-1, Sentinel-2, Landsat 8, and VIIRS nighttime satellites, as shown in Fig. 3. Each tile is of the size 800×800 pixels, with each corresponding to a 64 km^2 area. The EO data is then mapped into four classes, concerning the existence of human residents and the availability of the electricity supply.

2.9 Industry, Innovation, and Infrastructure (SDG-9)

Fostering industry, innovation, and infrastructure requires the development of sustainable, resilient systems that are responsive to environmental and societal challenges [69]. EO data can support these objectives by providing timely, spatially detailed insights into land use, urban growth, environmental conditions, and infrastructure health. Specifically, EO data enables smarter planning, risk assessment, and innovation in infrastructure design and industrial development, contributing to more sustainable and inclusive industrial growth. For example, detecting smoke plumes through satellite imagery can help monitor industrial emissions, offering valuable information for managing air quality and ensuring the continuity of critical infrastructure [70, 71, 72].

Therefore, the SustainFM dataset involves detecting the industrial smoke plumes from EO data based on the Smoke-Plume dataset [73]. The dataset acquires geographic locations of 624 sites from the European Pollutant Release and Transfer Register, which is a pollution reporting entity within the European Union. Subsequently, the dataset retrieved Sentinel-2 satellite imagery taken during 2019 for each site. Each raster image consists of all 12 spectral-band channels from the calibrated Level-2A reflectances and is cropped to a patch with a size of 120×120 pixels, corresponding to an area of $1.2 \times 1.2 \text{ km}^2$, as shown in Fig. 3. The dataset includes 21,350 images with 3,750 positive (a smoke plume is present) and 17,600 negative (no smoke plume is visible) samples. The dataset also generated masks indicating the pixels of smoke plumes for the positive images.

2.10 Reduced Inequalities (SDG-10)

Reducing inequality involves addressing income disparities, social exclusion, and unequal access to resources and services. Inequality often manifests spatially, with marginalized communities having poorer infrastructure and fewer services. Unequal access to sanitary services often leaves marginalized groups, such as low-income households, rural populations, and people living in informal settlements, without safe and dignified sanitation and threatens public health. EO provides an effective means to delineate these regions and analyze their socio-economic patterns, enabling the estimation of a continuous index that characterizes different degrees of deprivation [74].

SustainFM includes an analysis of the sanitation index (unequal access to sanitary services), based on the DHS survey dataset from SustainBench [43]. The dataset utilizes a cluster-level toilet index to represent the sanitation index, ranked on a 1 – 5 scale, where 5 is the “highest quality”. The dataset comprises a sanitation index for 89,271 clusters, computed from 2,143,329 households across 49 countries.

2.11 Sustainable Cities and Communities (SDG-11)

As urban populations surge, sustainable city development is crucial for managing infrastructure growth, mitigating environmental degradation, and ensuring equitable living conditions. Building construction serves as a key indicator of urban dynamics, reflecting shifts in population, economy, and land use. Monitoring these changes is essential for managing sustainable urban development. EO-based building change detection enables timely assessment of construc-

tion trends, informal settlements, and green space loss, informing urban planning, disaster response, and infrastructure equity [75, 76].

The SustainFM benchmark involves building change detection from remote sensing imagery based on the LEVIRCD dataset [77]. The LEVIRCD dataset focuses on significant land-use changes related to building, especially construction growth, spanning 5 to 14 years from 2002 to 2018 in the Texas region, U.S. It covers various types of buildings, such as villa residences, tall apartments, small garages and large warehouses. The dataset consists of 637 very high-resolution (VHR, 0.5 m/pixel) Google Earth (GE) image patch pairs, each with a size of 1024×1024 pixels. Annotations of building additions and removals encompass a diverse range of structures, including residential villas, high-rise apartments, garages, and warehouses. This supports spatially explicit modeling of urban growth for sustainable city planning.

2.12 Responsible Consumption and Production (SDG-12)

Promoting sustainable consumption and production is critical for reducing environmental impacts and conserving resources. Unsustainable practices, such as overextraction, waste mismanagement, and pollution, contribute to environmental degradation, which the EO data can accurately capture. Specifically, land use and land cover changes can provide a timely footprint on human activities, enabling the tracking of their responsibility. Meanwhile, multitemporal EO data offers a powerful means to monitor human activities, allowing for the dynamic tracking of land use changes linked to resource exploitation [78, 79, 80].

SustainFM addresses environmental degradation and conserves natural resources by monitoring changes caused by mining activities globally, based on the MineNetCD dataset [81]. As shown in Fig. 3, MineNetCD includes over 70,000 bitemporal image patches (256×256 pixels) from 100 global mining sites across six continents, collected via Google Earth Engine (GEE). Pixel-level change masks facilitate the assessment of mining expansion, supporting impact assessments and the pursuit of responsible production.

2.13 Climate Action (SDG-13)

Addressing climate change requires reducing greenhouse gas emissions, mitigating environmental degradation, and enhancing resilience to extreme weather events. EO data plays a crucial role in tracking climate variables, including land surface temperature, deforestation, and sea-level rise, as well as monitoring hazards such as floods, droughts, and wildfires [82]. In particular, mapping wildfires from satellite imagery provides spatial insight into fire frequency, intensity, and burn extent, informing carbon emission estimates and ecosystem recovery efforts [83, 84]. These data-driven insights support disaster preparedness and enable adaptive responses to climate-related risks.

The SustainFM benchmark includes a wildfire impact assessment task using the HLS Burn Scar Scenes dataset [85], as shown in Fig. 3. Based on the U.S. Monitoring Trends in Burn Severity (MTBS) database, this dataset combines burn scar shapefiles with Harmonized Landsat and Sentinel-2 (HLS) imagery acquired one to three months post-fire. It is created based on the Monitoring Trends in Burn Severity (MTBS) historical fire database, constructed in the U.S. region, which provides the location of wildfire emergence and the shape file of burn scars. It consists of 805 scenes, each measuring 512×512 pixels, with corresponding pixel-wise annotations of burn scars to support precise wildfire detection and post-event analysis.

2.14 Life below Water (SDG-14)

Safeguarding marine ecosystems requires urgent action to mitigate pollution and reduce anthropogenic stressors. EO provides a critical means of monitoring ocean health, enabling systematic assessment of sea surface temperature, chlorophyll concentration, turbidity, and harmful algal blooms. Moreover, EO can identify marine pollution ranging from oil slicks to plastic gyres, revealing eutrophication hotspots and floating debris to support early warning systems and targeted interventions [86, 87].

The SustainFM benchmark involves a task of detecting the marine debris and oil spill in the ocean based on the MADOS dataset [88], as shown in Fig. 3. It is composed of multispectral Sentinel-2 data, consisting of 174 scenes captured between 2015 and 2022, with approximately 1.5M annotated pixels, which are globally distributed and collected under various weather conditions. The dataset focuses on a wide range of classes of marine objects related to the pollutants in the form of marine debris and oil spills, which cover 4696 and 234,568 pixels. The dataset contains 2803 annotated image patches with a size of 240×240 , each covering an area of $2.4 \times 2.4 \text{ km}^2$.

Table 2: Overview of the foundation models for benchmarking.

Model	Architecture	Pretrained EO Data	Learning Strategies	Parameters (M)	Year
CROMA	ViT	SSL4EO-S12 [97]	Contrastive	396.13	2023
DOFA	ViT	DOFA [98]	MIM	178.20	2024
GFM-Swin	Swin-T	GeoPile [99]	MIM	128.36	2023
Prithvi	ViT	Prithvi-HLS [100]	MIM	153.28	2023
RemoteClip	ViT	SEG-4, DET-10, RET-3 [101]	Contrastive	154.34	2024
SatlasNet	Swin-T	SatlasPretrain [102]	Supervised	128.57	2023
ScaleMAE	ViT	FMoW-RGB [103]	MIM	396.21	2023
SpectralGPT	ViT	fMoW-S2 [103], BigEarthNet [104]	MIM	614.75	2024
SSL4EO-S12	ViT	SSL4EO-S12 [97]	MIM	61.99	2022
SoftCon	ViT	SSL4EO-S12 [97]	Contrastive	242.19	2024

2.15 Life on Land (SDG-15)

Protecting terrestrial ecosystems hinges on addressing threats from both natural and human activities. EO data is indispensable for tracking landscape dynamics, from shifts in vegetation cover and soil moisture to the aftermath of natural disasters [89]. Flood mapping via EO, for instance, enables rapid assessment of inundation impacts on forests, croplands, and habitats, which are vital for risk mitigation, restoration, and land stewardship [90, 91, 92].

SustainFM includes a flood detection task to advance disaster response and land management, which is built on the OMBRIA dataset [93], as shown in Fig. 3. This dataset integrates bitemporal, multimodal satellite data derived from Sentinel-1 SAR and Sentinel-2 multispectral imagery—paired with expert-labeled ground truth from ESA’s Copernicus Emergency Management Service. Covering 23 major flood events worldwide (2017–2021), OMBRIA comprises 3,376 annotated images (256×256 px).

2.16 Peace, Justice, and Strong Institutions (SDG-16)

Promoting peace, justice, and strong institutions requires protecting civilians, upholding human rights, and ensuring accountability during and after conflict. EO data contributes to these goals by enabling the classification and monitoring of war-induced damage to infrastructure, settlements, and cultural heritage sites [94]. High-resolution satellite imagery can detect changes such as building destruction, displaced populations, and disrupted land use, providing objective evidence in near real-time [95]. This information supports humanitarian response, aids in post-conflict reconstruction, and can serve as documentation for legal and human rights investigations.

SustainFM contains a task to detect war-related damage using the GAZADeepDAV dataset [96], which features eight-band PlanetScope images at 3m resolution (shown in Fig. 3). It comprises four pre- and four post-conflict scenes from Gaza in 2023, yielding 13,460 annotated patches (256×256 px), from which 7,264 were labeled as undamaged and 6,196 as damaged. GAZADeepDAV provides a distinctive foundation for developing EO tools that enhance transparency and resilience in conflict zones.

3 Geospatial Foundation Models

To ensure a rigorous and meaningful comparison, we follow PANGAEA [35] to select FMs by emphasizing reproducibility, methodological innovation, and scientific impact. Table 2 provides a comprehensive overview of the selected models, detailing their architectural scale, the datasets used for pretraining, and the associated EO sensors. These models represent diverse pretraining paradigms commonly employed in geospatial foundation modeling. Specifically, the selected FMs span three major pretraining strategies. (1) Contrastive learning leverages auxiliary data in an unsupervised manner, aligning representations across different modalities to learn robust and transferable features. (2) Masked image modeling (MIM) employs a self-supervised approach, where portions of the input (i.e., patches of an image) are masked and the model is trained to reconstruct the missing content, thereby learning semantically meaningful representations. (3) Supervised learning, by contrast, relies on labeled datasets to train the model directly for specific vision tasks, enabling the model to develop task-relevant perceptual capabilities. Below, we provide a detailed account of the ten FMs selected for evaluation, grouped according to their pretraining strategies: contrastive learning, masked image modeling, and supervised learning. These categories reflect the dominant paradigms currently shaping the development of general-purpose models in EO.

3.1 Contrastive Learning

Contrastive learning leverages auxiliary data in an unsupervised manner, aligning representations across different modalities to learn robust and transferable features [105]. This approach has shown particular promise in geospatial applications where multiple data modalities are naturally available.

CROMA [106] aligns geographically and temporally co-registered SAR-optical image pairs using a contrastive objective, while also incorporating unimodal MIM losses to enhance modality-specific representations. This dual approach enables the model to learn both cross-modal correspondences and modality-specific features, making it particularly effective for applications requiring integration of SAR and optical data.

RemoteCLIP [101] bridges the gap between vision and language by aligning satellite imagery with textual descriptions, resulting in visual representations enriched with high-level semantic concepts. By leveraging natural language descriptions, RemoteCLIP enables more intuitive interaction with geospatial data and supports zero-shot classification tasks based on textual queries.

SoftCon [107] introduces a multi-label supervision framework to learn cross-scene soft similarities, addressing challenges associated with rigid positive sample definitions and diverse semantic content in EO imagery. This approach recognizes that geospatial scenes often contain multiple land cover types and semantic concepts, requiring more nuanced similarity measures than traditional contrastive methods.

3.2 Masked Image Modeling

Masked image modeling employs a self-supervised approach, where portions of the input (i.e., patches of an image) are masked and the model is trained to reconstruct the missing content, thereby learning semantically meaningful representations [108, 109]. This strategy has been widely adopted in geospatial FMs due to its effectiveness in learning spatial patterns without requiring labeled data.

DOFA [98] employs dynamic spectral adaptation to pretrain on multimodal EO data, explicitly incorporating physical characteristics of spectral bands based on wavelength information. This physics-informed approach enables DOFA to better understand the relationships between different spectral channels and their physical meaning.

GFM-Swin [99] applies cross-sensor reconstruction to learn generalizable representations across EO modalities. By training on diverse sensor types, GFM-Swin develops robust features that transfer effectively across different imaging platforms and acquisition conditions.

Prithvi [100] is the first FM pretrained on Harmonized Landsat and Sentinel-2 (HLS) data from NASA, integrating temporal dynamics during pretraining to capture seasonality and land cover evolution. This temporal awareness makes Prithvi particularly suitable for applications requiring understanding of seasonal patterns and long-term environmental monitoring.

SpectralGPT [23] adapts MIM for multispectral imagery, incorporating domain-specific mechanisms to accommodate spectral data's unique structure and characteristics. The model leverages the sequential nature of spectral bands to improve reconstruction quality and learn more meaningful spectral representations.

ScaleMAE [110] addresses resolution heterogeneity in satellite data, learning robust representations from multimodal inputs at varying spatial scales. This multi-scale approach enables the model to handle the diverse resolution characteristics common in operational EO applications.

SSL4EO-S12 [97] serves as a foundational baseline FM, applying standard MIM techniques to Sentinel-1 and Sentinel-2 data in one of the earliest large-scale geospatial FM pretraining efforts. As one of the pioneering works in this field, SSL4EO-S12 established important benchmarks for subsequent geospatial FM development.

3.3 Supervised Learning

Supervised learning, by contrast, relies on labeled datasets to train the model directly for specific vision tasks, enabling the model to develop task-relevant perceptual capabilities. While requiring more annotated data, this approach can lead to highly specialized and effective models for specific application domains [19, 111].

SatlasNet [102] constructs a comprehensive multimodal dataset with diverse pretraining tasks, leveraging multi-task supervised learning to build an FM capable of capturing task-generalizable knowledge. By training simultaneously on multiple related tasks, SatlasNet develops rich representations that benefit from the complementary nature of different geospatial analysis objectives.

4 Evaluation

4.1 Implementation

The SustainFM benchmark involves a variety of datasets with diverse spectral features, resolutions, and image sizes, which are designed for different AI applications. This diversity presents challenges in evaluation. First, we preprocessed the dataset into a unified format to facilitate the data loading procedure for fine-tuning and testing the FMs. We resampled all the bands according to the highest resolution for the multispectral data, with different resolutions across the spectral bands. To ensure optimal performance and facilitate the convenient computation of AI algorithms, we crop the large-sized satellite images into small patches of approximately 256×256 . To ensure data transparency and reproducibility, all preprocessed datasets have been uploaded to the Huggingface platform, allowing them to be downloaded and reused within our implementation framework.

FMs adopt the pretraining-fine-tuning paradigm, with their pretrained encoders frozen and decoders fine-tuned on SDG-specific tasks. To ensure broad applicability, we attach task-specific decoders to FM encoders: UperNet for semantic segmentation, Siamese UperNet for change detection, and fully connected layers with global pooling for classification and regression. For the fine-tuning of FMs, cross-entropy loss is used for classification, segmentation, and change detection, while mean squared error (MSE) loss is applied for regression.

Despite the diversity in pretraining strategies, most FMs utilize transformer-based architectures, with a notable consideration of ViT [112]. Therefore, we adopt ViT as a baseline architecture to establish a performance reference. We train ViT from scratch on each subset of the SustainFM benchmark, treating it as a conventional deep learning model. Its performance is then compared against pre-trained and fine-tuned FMs. In addition, we include a traditional deep learning model, ResNet [113], as a representative of convolutional neural networks (CNNs), widely used for geospatial tasks over the past decade, as the second traditional model.

4.2 Accuracy Assessment

Table 3 presents the performance of various FMs (i.e., CROMA [106], RemoteCLIP [101], SoftCon [107], DOFA [98], GFM-Swin [99], Prithvi [100], SpectralGPT [23], ScaleMAE [110], SSL4EO-S12 [97], and SatlasNet [102]) and traditional deep models (i.e., ViT [112] and Resnet-50 [113]) across the SustainFM tasks. We report performance using the root mean square error (RMSE) for regression and the mean F1 score (mF1) for classification, capturing both the prediction of continuous values and the identification of categorical classes.

It can be seen that FMs generally exhibit superior performance across diverse tasks. This advantage stems from their ability to leverage large-scale pretraining, allowing them to adapt and generalize more effectively across various SDG challenges. Additionally, FMs converge faster in the training stage compared to traditional models, as their pretraining allows them to start with established knowledge, reducing the time and data needed for fine-tuning on SDG tasks. On the other hand, traditional models like ViT and ResNet-50, which are trained from scratch for each SDG task, may require more extensive tuning to achieve optimal performance, especially for broader generalization. However, traditional models remain competitive, particularly for task-specific applications where interpretability or fine-tuning on smaller datasets is essential. The decision between FMs and traditional models for SDG-related tasks ultimately depends on factors like model generalizability, the specificity of the task, and available computational resources, but we can highlight the evolving role of pretrained FMs in addressing the complex challenges of sustainable development. Furthermore, Fig. 3 provides a comprehensive model-wise comparison of the mean F1-score across five different datasets. Among the models, DOFA and GFM-Swin demonstrate strong, consistent performance across most datasets, with their F1-scores frequently reaching the upper range of the chart. The visualization also highlights model-specific strengths and weaknesses, such as the notable performance dip of the Prithvi model on the GloSoFarId dataset (red line), illustrating how a model’s effectiveness can vary significantly depending on the data to which it is applied.

4.3 Sustainability-Oriented Assessment

To assess different models’ environmental impact and sustainability, we employ the CodeCarbon library [114] to monitor energy consumption during training and inference, and show the results in Table 4. Specifically, we compare the energy footprint of decoder-only fine-tuning with full model fine-tuning, alongside the energy demands of baseline and traditional architectures (ViT and ResNet-50) trained from scratch. All models are evaluated on the OMBRIA dataset (Life on Land, SDG-15). In general, fine-tuning only the decoder of an FM can slightly boost performance while using less energy and producing lower CO₂ emissions than fine-tuning the entire model. This is because it requires fewer gradient computations and backpropagation steps. This relative difference varies substantially across all models, ranging from +40% to as much as +168%, as can be seen in the last column of Table 4, highlighting the considerable environmental benefits of updating only the decoder. For context, full fine-tuning of SpectralGPT

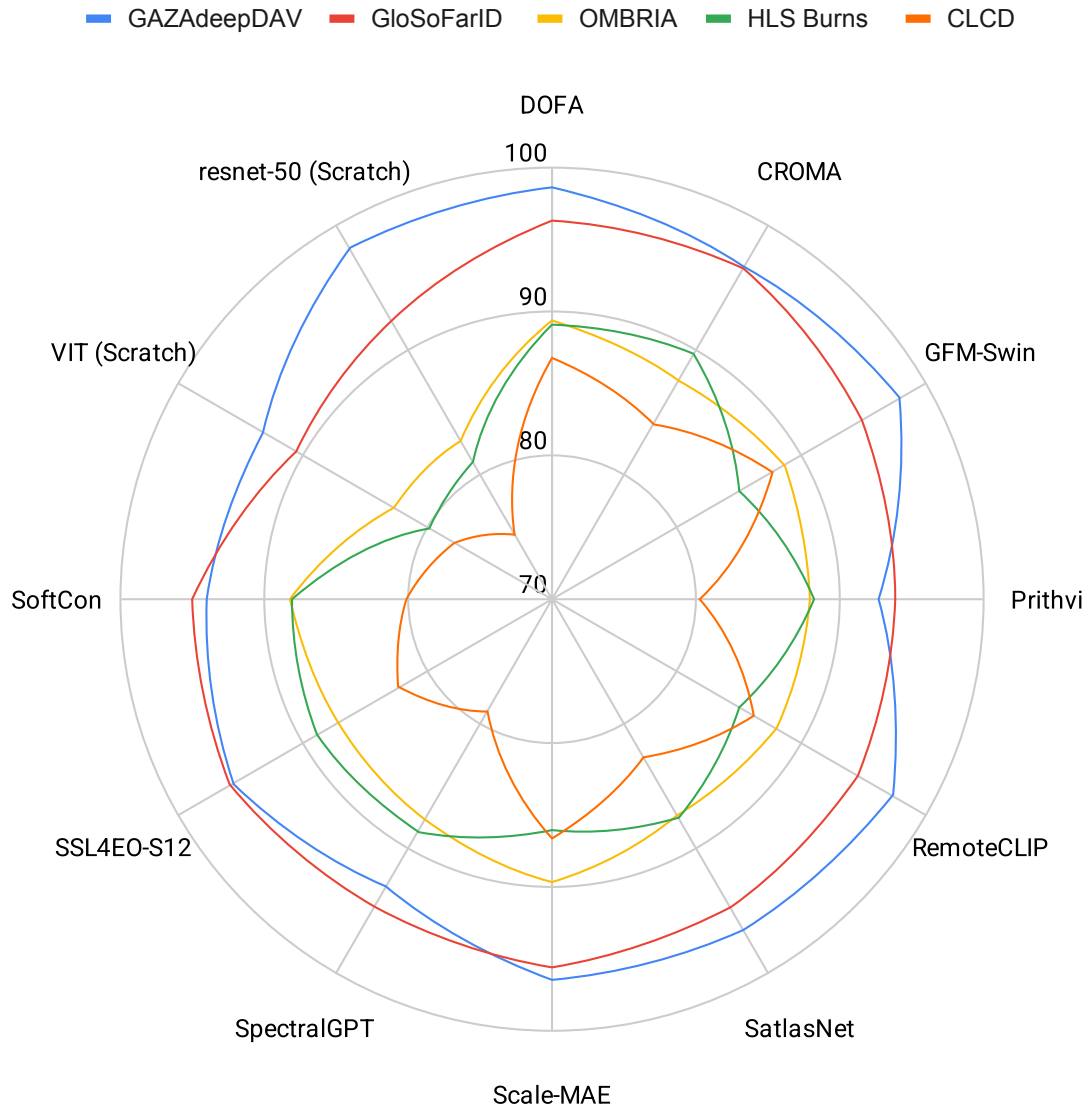
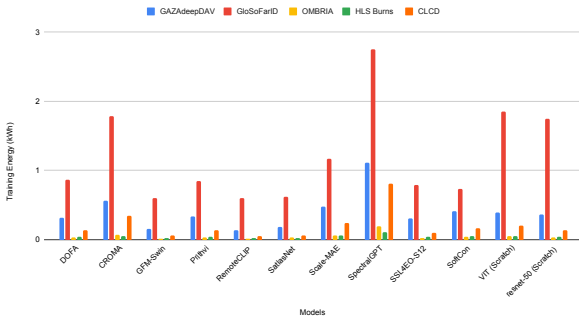
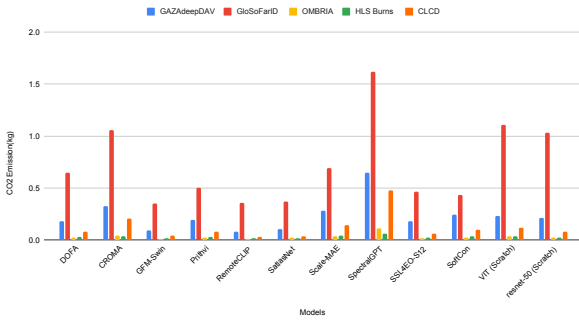
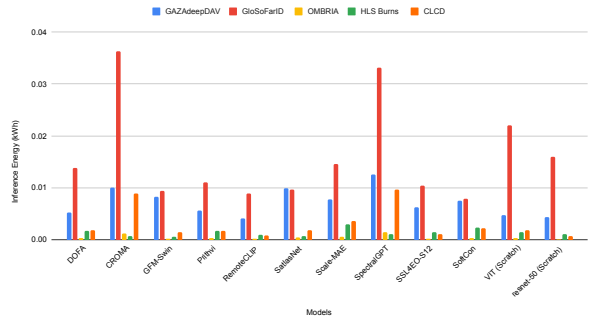


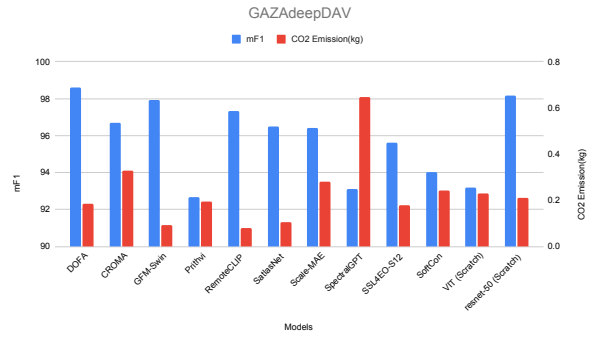
Figure 4: Model-wise comparison of mean F1-score across five datasets associated with different SDGs. This visualization highlights the performance differences among evaluated models, and provides insights into their generalization capabilities and robustness.



(a)



(g)



(h)

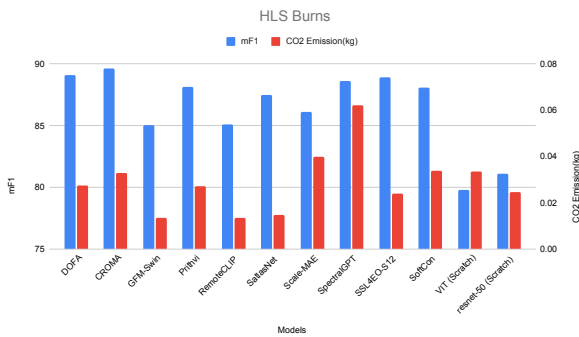
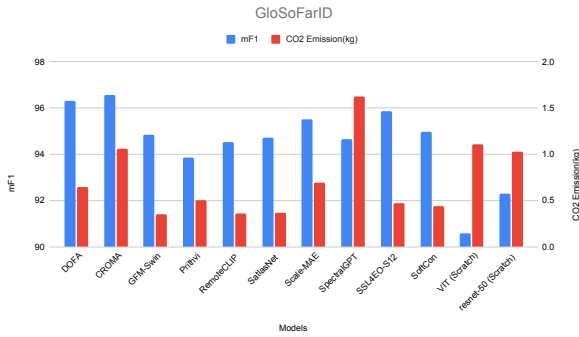


Figure 5: Comprehensive evaluation of energy efficiency, carbon footprint, and predictive performance across diverse models and datasets. (a) Training energy consumption in kWh, (b) inference energy consumption in kWh, and (c) associated CO₂ emissions in kg across all evaluated models. (d–h) Joint comparison of mF1 and CO₂ emissions for five representative datasets (GAZdeepDAV, GloSoFarID, Ombria, HLS Burns, and CLCD), illustrating the trade-off between model accuracy and environmental sustainability.

Table 3: Performance of Foundation Models and Traditional Methods across SustainFM tasks. Metrics are RMSE (\downarrow) or mF1 (\uparrow) as appropriate. The best performance per column is shown in **bold**, and the second-best is underlined. All results are calculated with 95% confidence interval, using bootstrapped per-sample means (10,000) bootstraps.

Model	#1	#2	#3	#4	#5	#6	#7	#8	#9	#10	#11	#12	#13	#14	#15	#16
	(\downarrow)	(\uparrow)	(\downarrow)	(\downarrow)	(\downarrow)	(\uparrow)	(\uparrow)	(\uparrow)	(\uparrow)	(\downarrow)	(\uparrow)					
CROMA	1.46	84.02	35.01	2.75	2.10	84.94	96.53	69.76	93.10	1.00	91.66	73.79	91.68	70.09	87.42	96.73
DOFA	1.42	<u>86.78</u>	34.91	2.85	2.07	<u>88.04</u>	<u>96.28</u>	72.96	93.86	1.03	<u>94.60</u>	80.70	<u>89.03</u>	<u>71.08</u>	<u>89.26</u>	<u>98.15</u>
GFM-Swin	1.39	87.69	34.74	2.71	<u>2.08</u>	87.89	94.83	75.82	93.58	1.04	93.78	78.06	84.55	72.42	88.54	97.93
Prithvi	1.45	80.18	34.94	3.00	2.38	83.99	93.85	69.85	91.60	1.06	91.33	69.13	88.13	53.50	87.79	92.67
RemoteCLIP	1.42	86.20	35.04	2.72	2.15	87.06	94.48	74.14	<u>95.00</u>	1.07	92.71	<u>79.29</u>	85.01	70.30	87.91	97.31
SatlasNet	1.42	82.67	34.97	2.79	2.14	82.14	94.73	70.04	93.09	1.01	92.32	73.79	87.51	63.88	87.42	96.50
Scale-MAE	1.48	86.49	34.77	3.04	2.17	88.34	95.54	69.07	94.68	1.10	95.00	77.16	86.03	61.39	89.64	96.40
SpectralGPT	<u>1.39</u>	78.97	<u>34.75</u>	<u>2.71</u>	2.16	79.29	94.70	<u>75.27</u>	93.91	1.04	91.41	71.73	90.07	62.54	87.58	93.12
SSL4EO-S12	1.44	82.20	34.90	2.75	2.34	83.29	95.85	69.15	93.65	0.96	91.25	70.49	88.78	64.34	87.02	95.62
SoftCon	1.39	79.97	34.79	2.74	2.13	81.34	94.94	70.02	91.16	<u>0.98</u>	91.56	68.03	88.03	53.37	88.12	93.98
ViT	1.50	77.72	34.81	2.89	2.20	74.29	90.58	59.91	93.17	1.10	92.73	74.52	79.17	34.56	82.61	93.17
ResNet-50	1.46	75.15	34.81	2.84	2.11	79.96	92.29	72.63	95.86	1.09	92.95	75.19	81.07	56.89	82.67	98.17

Table 4: Comparison of Finetuning the FM decoder only and Finetuning the Full Parameters. ViT and ResNet-50, the representatives of traditional deep learning models, are trained from scratch for SDG 15 (i.e., the OMBRIA dataset for flood mapping).

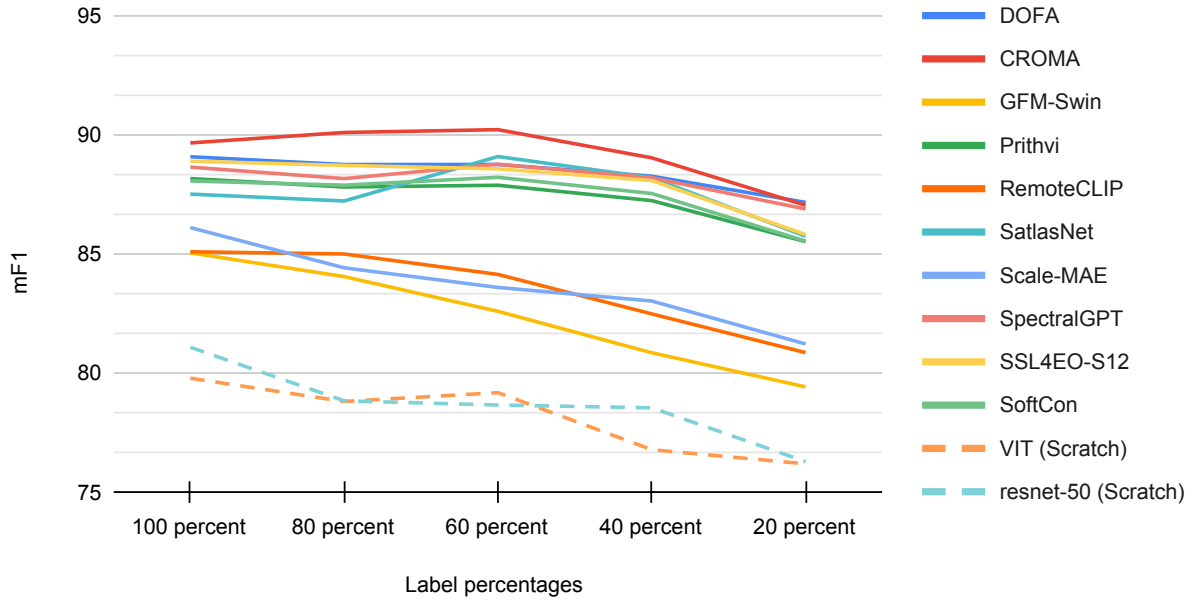
Model	Finetuning Decoder Only				Finetuning Full Parameters				CO ₂ Difference (%)
	mF1 \uparrow	Training Energy	Inference Energy	CO ₂ (kg)	mF1 \uparrow	Training Energy	Inference Energy	CO ₂ (kg)	
CROMA	87.42	0.07424	0.00118	0.04410	88.03	0.10406	0.00122	0.06150	+46.68
DOFA	89.26	0.03590	0.00029	0.02121	89.46	0.05288	0.00029	0.03111	+39.46
GFM-Swin	88.54	0.01766	0.00021	0.01077	89.55	0.04023	0.00022	0.02373	+120.33
Prithvi	87.91	0.03473	0.00029	0.02104	87.63	0.05246	0.00028	0.03071	+61.11
RemoteCLIP	87.79	0.01497	0.00014	0.00918	87.51	0.02500	0.00018	0.01479	+61.11
SatlasNet	87.34	0.03428	0.00041	0.02028	88.97	0.09296	0.00040	0.05436	+168.05
Scale-MAE	89.64	0.05802	0.00052	0.03393	89.63	0.11246	0.00057	0.06605	+94.67
SpectralGPT	87.58	0.19017	0.00142	0.11206	87.95	0.45666	0.00160	0.26864	+139.73
SSL4EO-S12	87.02	0.02355	0.00018	0.01421	87.80	0.03371	0.00019	0.01990	+40.04
SoftCon	88.12	0.04170	0.00033	0.02498	88.16	0.06883	0.00041	0.04055	+62.33
					Trained from Scratch for traditional deep models				
ViT	-	-	-	-	82.61	0.05345	0.00031	0.03293	-
ResNet-50	-	-	-	-	82.67	0.03782	0.00011	0.02346	-

produces around 270g of CO₂ emissions. This is roughly equivalent to driving a car for 0.7 miles, or less than 1% of the average American’s daily per-person emissions (39 kg/day) [115]. Complete training for traditional deep learning models usually results in higher energy consumption and CO₂ emissions compared to partially fine-tuned FMs, since conventional models require training from scratch on large datasets over many iterations. In contrast, FMs benefit from pretraining on diverse data; They can be adapted to downstream tasks using a small amount of labeled data and fewer updates, which makes them more energy-efficient and scalable in the long run.

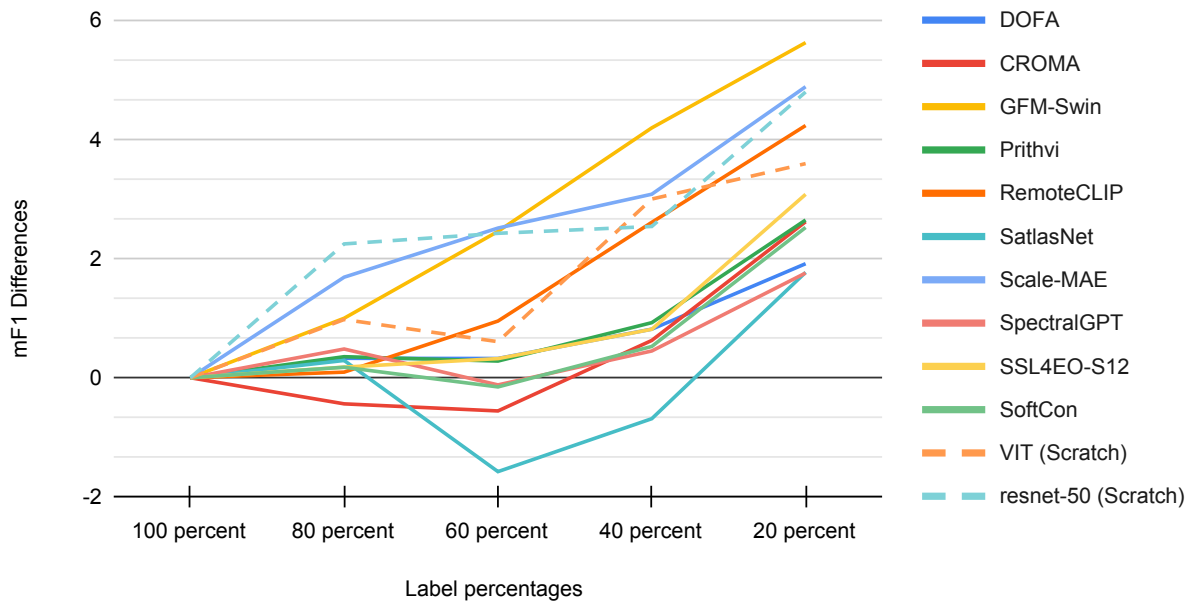
For a fair comparison across different methods and datasets, Fig. 5 presents a comprehensive evaluation of models along three key dimensions: predictive performance, energy consumption, and carbon footprint. The analysis reveals a significant trade-off between model accuracy and environmental impact, which is heavily influenced by the chosen dataset. Notably, the GloSoFarId dataset consistently requires the most energy for both training and inference, leading to CO₂ emissions that are an order of magnitude higher than all other datasets. While some models, such as SpectralGPT, achieve competitive performance at a substantial environmental cost, others, like DOFA and GFM-Swin, demonstrate a more favorable balance of high mF1 scores and lower carbon footprints. High emissions are also observed for the CROMA and ViT (Scratch) models on the same dataset. In contrast, the HLS Burns and CLCD datasets result in significantly lower emissions across all models. This work highlights the critical need to expand model evaluation frameworks beyond traditional performance metrics to include the full energy and environmental costs.

Fig. 6 illustrates the impact of reducing training data on the performance of various models when applied to the HLS Burns dataset. As the percentage of labeled training data is progressively reduced from 100% down to 20%, a general downward trend exists for all models, indicating that a decrease in training data leads to a decline in performance. Models like GFM-Swin and DOFA maintain relatively high scores, while others like ViT (Scratch) and resnet-50 (Scratch) experience a more pronounced performance drop. Fig. 6(b) provides a more focused view of model robustness by plotting the absolute difference in mF1 score relative to the full (100%) training set. It reveals that GFM-Swin and DOFA are the most robust models, as their mF1 scores decrease only slightly. Conversely, models like Spectral-

GPT and Scale-MAE show the largest performance degradation, indicating that they are more sensitive to the amount of labeled training data.



(a)



(b)

Figure 6: Impact of training data reduction on model performance for HLS Burns. (a) mF1 scores achieved by each model when trained on progressively reduced subsets of the training data, compared to full training (100%). (b) Absolute differences in mF1 scores between full training and reduced-sample settings, highlighting model robustness to limited labeled data.

Table 5: Comparison between Foundation Models (decoder fine-tuned) and Traditional Deep Models (trained from scratch), across performance, efficiency, and sustainability metrics. Color-coded markers indicate relative performance: ✓best, ✓competitive, and ✗ limitation.

Assessment Criteria	FMs (Decoder Fine-tuned)	Traditional Models
Model Performance (mF1)	✓high across models	✗ lower performance
Training Efficiency (kWh)	✓lower training cost	✓moderate
Inference Efficiency (kWh/sample)	✓low in most cases	✓competitive (ResNet-50)
CO ₂ Emissions (kg)	✓generally low	✓moderate
Data Efficiency	✓few-shot fine-tuning	✗ requires full retraining
Generalization across tasks	✓broad task adaptability	✗ narrower scope
Convergence Speed	✓faster, low compute	✗ slower convergence

5 Discussions

Table 5 summarizes the strengths and weaknesses of FMs (decoder fine-tuned) compared to traditional models in terms of performance, efficiency, and sustainability criteria. Here, we discuss our key findings, as well as principles and considerations for geospatial FMs. Overall, foundation models demonstrate clear advantages in terms of model performance, data efficiency, convergence speed, and generalization capability. They achieve higher mF1 scores with substantially lower training costs and CO₂ emissions, reflecting both computational and environmental benefits. Moreover, their few-shot fine-tuning capability enables rapid adaptation to diverse downstream tasks, contrasting with the full retraining requirements of traditional models. While traditional models such as ResNet-50 remain competitive in inference efficiency, their overall scope and scalability are limited. These results highlight the superior efficiency and adaptability of foundation models for sustainable and general-purpose Earth observation tasks.

5.1 Key Findings

- **FMs deliver strong performance, but are not always superior to traditional approaches.** Our results indicate that it is impossible to make a universal claim about the superiority of FMs over traditional deep learning models (e.g., ViT) in terms of accuracy. Performance varies depending on the dataset, task, and fine-tuning strategy. Nonetheless, in many of our experiments, FMs outperformed their traditional counterparts.
- **Transferability offers a step toward energy-efficient AI across domains.** A commonly held belief is that FMs are inherently resource-intensive. However, our results suggest a more balanced picture. Once pretrained, FMs can be fine-tuned with minimal labeled data, which offers an energy-efficient alternative to training models from scratch. This transferability makes them especially attractive for zero-shot or few-shot learning scenarios, where resource constraints or data scarcity are significant limitations.
- **FMs enable scalable solutions for global sustainability.** One of the most promising aspects of FMs is their potential to serve as general-purpose tools across geospatial applications. Their ability to generalize across regions, tasks, and modalities makes them particularly suited to addressing complex, large-scale problems related to the SDGs. This cross-domain flexibility allows broader, interdisciplinary adoption among scientists and practitioners.
- **High generalization and fast convergence make FMs a scalable alternative to traditional models.** Traditional deep learning models typically require task-specific training from scratch to achieve competitive performance, which results in considerable computational and energy costs for each new use case. In contrast, FMs exhibit strong generalization capabilities across various tasks, often requiring only minimal fine-tuning. This enables faster convergence and lower overall resource consumption in the long term.

5.2 Best Practices

- **Energy efficiency and transparency in FM training:** Training FMs from scratch requires an enormous amount of time and computational resources, which make it largely impractical for benchmarking studies like ours. Given these constraints, we focused on fine-tuning existing pre-trained models. Accordingly, the energy use reported in our work reflects only this fine-tuning phase. We strongly encourage researchers to

clearly report CO₂ emissions or other environmental impact measures whenever they introduce new FMs to provide the whole picture. This transparency is essential to support responsible AI development and help the community move toward more sustainable practices in training and using large models.

- **Aligning models with the nature of EO:** The development of geospatial FMs demands a methodological shift that reflects the unique nature of EO data. As argued in [116], EO data is not just another visual modality; They include unique properties, such as spectral and temporal richness, geolocation, physical constraints, and sensor-specific noise patterns, which are not adequately addressed by conventional vision-based pretraining objectives such as masked image modeling or contrastive learning or the models themselves [117]. As a result, downstream geospatial tasks such as change detection, time-series forecasting, and biophysical retrieval may suffer from a misalignment between model pretraining and real-world task demands. Moreover, relying on standard computer vision architectures, such as UperNet or Siamese UperNet, can hide the real impact of task-specific reasoning in geospatial applications. To move the field forward, we advocate for models that capture the specific nature of geospatial data. This includes using physics-informed pretraining that brings in domain knowledge, learning methods that combine different types of data (like spatial, spectral, and temporal), and flexible decoder designs with suitable loss functions that match the needs of specific geospatial tasks.
- **Scaling laws for geospatial FMs:** Furthermore, the importance of scale must not be overlooked. Though originally developed for language models, scaling laws emphasize the importance of maintaining an appropriate data-to-parameter ratio, typically ranging from 5:1 to 20:1, to achieve generalizable performance [118]. As highlighted in [117], many geospatial FMs are undertrained relative to their size, limiting their generalization capacity despite architectural scale. Smaller models risk underfitting complex Earth patterns, while larger models require correspondingly large and diverse training datasets to fulfill their potential.
- **Responsible practices with building fair and sustainable models:** The environmental and ethical responsibilities tied to geospatial FM development are substantial. The carbon footprint of model training, particularly for large-scale architectures, remains a concern, especially when models are trained without transparent reporting. Moreover, EO datasets often contain geographic, sensor-based, and socioeconomic imbalances, which can propagate biases into model predictions [32]. These biases risk producing results that are not representative of the true situation. Mitigation strategies include careful data curation, geographic rebalancing, and inclusive benchmarking practices.
- **Beyond benchmarking toward real-world impact:** Last but not least, we want to emphasize that while technical benchmarking is a necessary step, it is not a sufficient one. Public perceptions significantly influence policy decisions by shaping political priorities, public support, and the feasibility of implementation. Performance metrics alone do not guarantee real-world relevance or societal impact. While benchmarks offer a standardized way to measure methodological progress, they must be grounded in broader, mission-driven goals. As aligned with studies such as [119], the impactful deployment of geospatial FMs, especially in support of SDG-17, relies on collaboration with stakeholders, domain experts, and decision-makers who can translate model outputs into actionable insights for "Becoming Good at AI for Good". In practice, benchmarking and modeling represent just two components of a complete solution. Defining relevant problems, selecting appropriate metrics, involving domain experts, and clearly articulating the model's purpose are equally important. FMs, unlike narrow models that suffer from "catastrophic forgetting", offer unique advantages for long-term monitoring and adaptation to temporal shifts in the Earth system. Well-pretrained FMs enable lifelong learning and can generalize to new tasks with minimal further tuning.

The regulation of FMs varies globally. The EU's AI Act (2024) introduces the first binding framework focused on risk management and transparency, classifying large models ($> 10^{25}$ FLOPs) as systemically risky. The U.S. Executive Order 14110 (2023) adopts a flexible, security-oriented approach, while China's 2023 Measures emphasize content labeling and safety reviews. The UK favors principles-based innovation, and Canada's AIDA provides a balanced model with targeted obligations for high-impact systems.

Together, these differing regulatory approaches illustrate both the complexity and the promise of global AI governance. The divergence is not only a legal matter, but it also influences where innovation occurs and who benefits from it. Yet, within this diversity lies a chance to build a more balanced and trustworthy global AI ecosystem. Through open dialogue, shared standards, and mutual learning, countries can turn regulatory variation into a driver of collective progress rather than fragmentation.

If shaped by cooperation, transparency, and ethical responsibility, emerging governance frameworks can strengthen public trust, improve data stewardship, and support international collaboration. To realize the potential of foundation models for the SDGs (from equitable access to education and healthcare to climate resilience and social inclusion), governance must evolve toward systems that are interoperable, transparent, and human-centered. Aligning oversight with shared principles of openness, accountability, and social benefit can ensure that the next generation of founda-

tion models becomes not only a technological advance, but also a genuine force for sustainable and inclusive global progress.

6 Conclusion

In this study, we establish a comprehensive benchmark that integrates mainstream Foundation Models with multi-source datasets aligned with SDG objectives, enabling systematic evaluation of their true societal value and practical utility in supporting global sustainable development. Through systematic evaluation across key criteria, including transferability, data efficiency, energy costs, and operational impact, we provide a grounded, rigorous assessment that challenges assumptions and clarifies the actual added value, if any, of FMs in this domain. By moving beyond traditional accuracy metrics to include transferability, energy efficiency, and operational impact, this work addresses the urgent need for AI solutions that demonstrably contribute to global sustainability. Ultimately, our goal is to contribute to global sustainability objectives and promote social good, a key aspect that has been undermined in many current geospatial FMs.

Geospatial FMs can make EO more accessible, actionable, and relevant by combining innovative methodologies with impactful applications and deep domain expertise. Future FMs will help to address global challenges and advance the SDGs. FMs can deliver actionable insights for sustainable development, humanitarian response, and environmental conservation if designed responsibly, i.e., with attention to energy efficiency, open-access datasets, and a strong emphasis on transparency and inclusivity—geospatial. By democratizing access to AI resources (e.g., input data, curated datasets, model architectures, and pretrained weights), geospatial FMs can reduce disparities in dataset availability and empower stakeholders as a key driver of innovation to foster global progress toward sustainability.

References

- [1] M. Burke, A. Driscoll, D. B. Lobell, and S. Ermon, “Using satellite imagery to understand and promote sustainable development,” *Science*, vol. 371, no. 6535, p. eabe8628, 2021.
- [2] U. N. DPI, *The sustainable development goals*. Stylus Publishing, LLC, 2017.
- [3] J. D. Sachs, G. Schmidt-Traub, M. Mazzucato, D. Messner, N. Nakicenovic, and J. Rockström, “Six transformations to achieve the sustainable development goals,” *Nature sustainability*, vol. 2, no. 9, pp. 805–814, 2019.
- [4] T. Hák, S. Janoušková, and B. Moldan, “Sustainable development goals: A need for relevant indicators,” *Ecological indicators*, vol. 60, pp. 565–573, 2016.
- [5] S. Sorooshian, “The sustainable development goals of the united nations: A comparative midterm research review,” *Journal of Cleaner Production*, vol. 453, p. 142272, 2024.
- [6] A. Kavvada, G. Metternicht, F. Kerblat, N. Mudau, M. Haldorson, S. Laldaparsad, L. Friedl, A. Held, and E. Chuvieco, “Towards delivering on the sustainable development goals using earth observations,” *Remote sensing of environment*, vol. 247, p. 111930, 2020.
- [7] C. Persello, J. D. Wegner, R. Hänsch, D. Tuia, P. Ghamisi, M. Koeva, and G. Camps-Valls, “Deep learning and Earth observation to support the Sustainable Development Goals: Current approaches, open challenges, and future opportunities,” *IEEE Geoscience and Remote Sensing Magazine*, vol. 10, no. 2, pp. 172–200, 2022.
- [8] R. Vinuesa, H. Azizpour, I. Leite, M. Balaam, V. Dignum, S. Domisch, A. Felländer, S. D. Langhans, M. Tegmark, and F. Fuso Nerini, “The role of artificial intelligence in achieving the sustainable development goals,” *Nature communications*, vol. 11, no. 1, p. 233, 2020.
- [9] G. Camps-Valls, M.-Á. Fernández-Torres, K.-H. Cohrs, A. Höhl, A. Castelletti, A. Pacal, C. Robin, F. Martinuzzi, I. Papoutsis, I. Prapas *et al.*, “Artificial intelligence for modeling and understanding extreme weather and climate events,” *Nature Communications*, vol. 16, no. 1, p. 1919, 2025.
- [10] D. Tamayo-Vera, M. Mesbah, Y. Zhang, and X. Wang, “Advanced machine learning for regional potato yield prediction: analysis of essential drivers,” *npj Sustainable Agriculture*, vol. 3, no. 1, p. 12, 2025.
- [11] N. Ratledge, G. Cadamuro, B. De La Cuesta, M. Stigler, and M. Burke, “Using machine learning to assess the livelihood impact of electricity access,” *Nature*, vol. 611, no. 7936, pp. 491–495, 2022.
- [12] K. Hughes, H. Sharma, P. Priyadarshini, T. Vågen, L. Winowiecki, and R. Meinzen-Dick, “Integrating Earth observation, biophysical, and survey data to evaluate the ecological impacts of a common land protection and restoration intervention in rajasthan, india,” *Humanities and Social Sciences Communications*, vol. 11, no. 1, pp. 1–9, 2024.

- [13] Q. Zhao and L. Yu, "Advancing sustainable development goals through earth observation satellite data: Current insights and future directions," *Journal of Remote Sensing*, vol. 5, p. 0403, 2025.
- [14] B. Ferreira, M. Iten, and R. G. Silva, "Monitoring sustainable development by means of earth observation data and machine learning: A review," *Environmental Sciences Europe*, vol. 32, no. 1, pp. 1–17, 2020.
- [15] P. Ghamisi, B. Rasti, N. Yokoya, Q. Wang, B. Hofle, L. Bruzzone, F. Bovolo, M. Chi, K. Anders, R. Gloaguen *et al.*, "Multisource and multitemporal data fusion in remote sensing: A comprehensive review of the state of the art," *IEEE Geoscience and Remote Sensing Magazine*, vol. 7, no. 1, pp. 6–39, 2019.
- [16] H. Zhang, J.-J. Xu, H.-W. Cui, L. Li, Y. Yang, C.-S. Tang, and N. Boers, "When geoscience meets foundation models: Toward a general geoscience artificial intelligence system," *IEEE geoscience and remote sensing magazine*, 2024.
- [17] A. Xiao, W. Xuan, J. Wang, J. Huang, D. Tao, S. Lu, and N. Yokoya, "Foundation models for remote sensing and earth observation: A survey," *IEEE Geoscience and Remote Sensing Magazine*, 2025.
- [18] H. Xu, C. Zhang, P. Yue, and K. Wang, "Sdcluster: A clustering based self-supervised pre-training method for semantic segmentation of remote sensing images," *ISPRS Journal of Photogrammetry and Remote Sensing*, vol. 223, pp. 1–14, 2025.
- [19] D. Wang, Q. Zhang, Y. Xu, J. Zhang, B. Du, D. Tao, and L. Zhang, "Advancing plain vision transformer toward remote sensing foundation model," *IEEE Transactions on Geoscience and Remote Sensing*, vol. 61, pp. 1–15, 2022.
- [20] X. Wang, X. Zhang, Y. Cao, W. Wang, C. Shen, and T. Huang, "Seggpt: Towards segmenting everything in context," in *Proceedings of the IEEE/CVF International Conference on Computer Vision*, 2023, pp. 1130–1140.
- [21] M. Oquab, T. Darcet, T. Moutakanni, H. Vo, M. Szafraniec, V. Khalidov, P. Fernandez, D. Haziza, F. Massa, A. El-Nouby *et al.*, "Dinov2: Learning robust visual features without supervision," *arXiv preprint arXiv:2304.07193*, 2023.
- [22] S. Lu, J. Guo, J. R. Zimmer-Dauphinee, J. M. Nieuwsma, X. Wang, S. A. Wernke, Y. Huo *et al.*, "Vision foundation models in remote sensing: A survey," *IEEE Geoscience and Remote Sensing Magazine*, 2025.
- [23] D. Hong, B. Zhang, X. Li, Y. Li, C. Li, J. Yao, N. Yokoya, H. Li, P. Ghamisi, X. Jia *et al.*, "SpectralGPT: Spectral remote sensing foundation model," *IEEE Transactions on Pattern Analysis and Machine Intelligence*, 2024.
- [24] X. Sun, P. Wang, W. Lu, Z. Zhu, X. Lu, Q. He, J. Li, X. Rong, Z. Yang, H. Chang *et al.*, "RingMo: A remote sensing foundation model with masked image modeling," *IEEE Transactions on Geoscience and Remote Sensing*, vol. 61, pp. 1–22, 2022.
- [25] X. Li, D. Hong, and J. Chanussot, "S2MAE: A spatial-spectral pretraining foundation model for spectral remote sensing data," in *Proceedings of the IEEE/CVF Conference on Computer Vision and Pattern Recognition*, 2024, pp. 24 088–24 097.
- [26] X. Guo, J. Lao, B. Dang, Y. Zhang, L. Yu, L. Ru, L. Zhong, Z. Huang, K. Wu, D. Hu *et al.*, "Skysense: A multi-modal remote sensing foundation model towards universal interpretation for Earth observation imagery," in *Proceedings of the IEEE/CVF Conference on Computer Vision and Pattern Recognition*, 2024, pp. 27 672–27 683.
- [27] W. Zhang, M. Cai, T. Zhang, Y. Zhuang, and X. Mao, "EarthGPT: A universal multi-modal large language model for multi-sensor image comprehension in remote sensing domain," *IEEE Transactions on Geoscience and Remote Sensing*, 2024.
- [28] V. Nedungadi, A. Kariryaa, S. Oehmcke, S. Belongie, C. Igel, and N. Lang, "MMEarth: Exploring multi-modal pretext tasks for geospatial representation learning," in *European Conference on Computer Vision*. Springer, 2024, pp. 164–182.
- [29] X. Li, C. Li, P. Ghamisi, and D. Hong, "Fleximo: A flexible remote sensing foundation model," *arXiv preprint arXiv:2503.23844*, 2025.
- [30] Y. Wang, H. H. Hernández, C. M. Albrecht, and X. X. Zhu, "Feature guided masked autoencoder for self-supervised learning in remote sensing," *IEEE Journal of Selected Topics in Applied Earth Observations and Remote Sensing*, vol. 18, pp. 321–336, 2025.
- [31] K. Wu, Y. Zhang, L. Ru, B. Dang, J. Lao, L. Yu, J. Luo, Z. Zhu, Y. Sun, J. Zhang *et al.*, "A semantic-enhanced multi-modal remote sensing foundation model for earth observation," *Nature Machine Intelligence*, pp. 1–15, 2025.

- [32] P. Ghamisi, W. Yu, A. Marinoni, C. M. Gevaert, C. Persello, S. Selvakumaran, M. Girotto, B. P. Horton, P. Rufin, P. Hostert *et al.*, “Responsible artificial intelligence for Earth observation: Achievable and realistic paths to serve the collective good,” *IEEE Geoscience and Remote Sensing Magazine*, 2025.
- [33] A. Lacoste, N. Lehmann, P. Rodriguez, E. Sherwin, H. Kerner, B. Lütjens, J. Irvin, D. Dao, H. Alemohammad, A. Drouin *et al.*, “Geo-bench: Toward foundation models for earth monitoring,” *Advances in Neural Information Processing Systems*, vol. 36, pp. 51 080–51 093, 2023.
- [34] N. Dionelis, C. Fibaek, L. Camilleri, A. Luyts, J. Bosmans, and B. L. Saux, “Evaluating and benchmarking foundation models for earth observation and geospatial ai,” *arXiv preprint arXiv:2406.18295*, 2024.
- [35] V. Marsocci, Y. Jia, G. L. Bellier, D. Kerekes, L. Zeng, S. Hafner, S. Gerard, E. Brune, R. Yadav, A. Shibli *et al.*, “PANGAEA: A global and inclusive benchmark for geospatial foundation models,” *arXiv preprint arXiv:2412.04204*, 2024.
- [36] P. Radanliev, O. Santos, A. Brandon-Jones, and A. Joinson, “Ethics and responsible ai deployment,” *Frontiers in Artificial Intelligence*, vol. 7, p. 1377011, 2024.
- [37] A. Tassa, S. Willekens, A. Lahcen, L. Laurich, and C. Mathieu, “On-going european space agency activities on measuring the benefits of earth observations to society: Challenges, achievements and next steps,” *Frontiers in Environmental Science*, vol. 10, p. 788843, 2022.
- [38] J. Van Den Hoek and H. K. Friedrich, “Satellite-based human settlement datasets inadequately detect refugee settlements: a critical assessment at thirty refugee settlements in uganda,” *Remote Sensing*, vol. 13, no. 18, p. 3574, 2021.
- [39] F. Cigna and D. Tapete, “Urban growth and land subsidence: Multi-decadal investigation using human settlement data and satellite insar in morelia, mexico,” *Science of the total Environment*, vol. 811, p. 152211, 2022.
- [40] M. Pesaresi, M. Schiavina, P. Politis, S. Freire, K. Krasnodebska, J. H. Uhl, A. Carioli, C. Corbane, L. Dijkstra, P. Florio *et al.*, “Advances on the global human settlement layer by joint assessment of earth observation and population survey data,” *International Journal of Digital Earth*, vol. 17, no. 1, p. 2390454, 2024.
- [41] M. E. Brown, K. Grace, G. Shively, K. B. Johnson, and M. Carroll, “Using satellite remote sensing and household survey data to assess human health and nutrition response to environmental change,” *Population and environment*, vol. 36, no. 1, pp. 48–72, 2014.
- [42] M. Sharma, F. Yang, D.-N. Vo, E. Suel, S. Mishra, S. Bhatt, O. Fiala, W. Rudgard, and S. Flaxman, “KidSat: satellite imagery to map childhood poverty dataset and benchmark,” *arXiv preprint arXiv:2407.05986*, 2024.
- [43] C. Yeh, C. Meng, S. Wang, A. Driscoll, E. Rozi, P. Liu, J. Lee, M. Burke, D. Lobell, and S. Ermon, “SustainBench: Benchmarks for monitoring the sustainable development goals with machine learning,” in *Thirty-fifth Conference on Neural Information Processing Systems, Datasets and Benchmarks Track (Round 2)*, 12 2021. [Online]. Available: <https://openreview.net/forum?id=5HR3vCylqD>
- [44] K. E. Joyce, S. E. Belliss, S. V. Samsonov, S. J. McNeill, and P. J. Glassey, “A review of the status of satellite remote sensing and image processing techniques for mapping natural hazards and disasters,” *Progress in physical geography*, vol. 33, no. 2, pp. 183–207, 2009.
- [45] Y. Jiang, Z. Lu, S. Li, Y. Lei, Q. Chu, X. Yin, and F. Chen, “Large-scale and high-resolution crop mapping in china using sentinel-2 satellite imagery,” *Agriculture*, vol. 10, no. 10, p. 433, 2020.
- [46] H. Müller, P. Rufin, P. Griffiths, A. J. B. Siqueira, and P. Hostert, “Mining dense landsat time series for separating cropland and pasture in a heterogeneous brazilian savanna landscape,” *Remote Sensing of Environment*, vol. 156, pp. 490–499, 2015.
- [47] T. Garnett, M. C. Appleby, A. Balmford, I. J. Bateman, T. G. Benton, P. Bloomer, B. Burlingame, M. Dawkins, L. Dolan, D. Fraser *et al.*, “Sustainable intensification in agriculture: premises and policies,” *Science*, vol. 341, no. 6141, pp. 33–34, 2013.
- [48] M. Liu, Z. Chai, H. Deng, and R. Liu, “A cnn-transformer network with multiscale context aggregation for fine-grained cropland change detection,” *IEEE Journal of Selected Topics in Applied Earth Observations and Remote Sensing*, vol. 15, pp. 4297–4306, 2022.
- [49] T. E. Ford, R. R. Colwell, J. B. Rose, S. S. Morse, D. J. Rogers, and T. L. Yates, “Using satellite images of environmental changes to predict infectious disease outbreaks,” *Emerging infectious diseases*, vol. 15, no. 9, p. 1341, 2009.
- [50] K. Hu, X. Yang, J. Zhong, F. Fei, and J. Qi, “Spatially explicit mapping of heat health risk utilizing environmental and socioeconomic data,” *Environmental Science & Technology*, vol. 51, no. 3, pp. 1498–1507, 2017.

- [51] Q. Chen, M. Ding, X. Yang, K. Hu, and J. Qi, "Spatially explicit assessment of heat health risk by using multi-sensor remote sensing images and socioeconomic data in yangtze river delta, china," *International Journal of Health Geographics*, vol. 17, no. 1, p. 15, 2018.
- [52] D. Runfola, A. Stefanidis, and H. Baier, "Using satellite data and deep learning to estimate educational outcomes in data-sparse environments," *Remote Sensing Letters*, vol. 13, no. 1, pp. 87–97, 2022.
- [53] A. Andries, S. Morse, R. J. Murphy, J. Lynch, and E. R. Woolliams, "Assessing education from space: Using satellite earth observation to quantify overcrowding in primary schools in rural areas of nigeria," *Sustainability*, vol. 14, no. 3, p. 1408, 2022.
- [54] A. Maharana and E. O. Nsoesie, "Use of deep learning to examine the association of the built environment with prevalence of neighborhood adult obesity," *JAMA network open*, vol. 1, no. 4, pp. e181 535–e181 535, 2018.
- [55] B. M. Dahu, S. Khan, I. E. Toubal, M. Alshehri, C. I. Martinez-Villar, O. B. Ogundele, L. R. Sheets, and G. J. Scott, "Geospatial modeling of deep neural visual features for predicting obesity prevalence in missouri: Quantitative study," *JMIR AI*, vol. 3, no. 1, p. e64362, 2024.
- [56] J. Cao, Q. Sun, D. Zhao, M. Xu, Q. Shen, D. Wang, Y. Wang, and S. Ding, "A critical review of the appearance of black-odorous waterbodies in china and treatment methods," *Journal of hazardous materials*, vol. 385, p. 121511, 2020.
- [57] M. Modiegi, I. T. Rampedi, and S. G. Tesfamichael, "Comparison of multi-source satellite data for quantifying water quality parameters in a mining environment," *Journal of Hydrology*, vol. 591, p. 125322, 2020.
- [58] S. Balakrishnan, P. M. Preetam Raj, J. Somasekar, K. V. Kumar, S. Amutha, and A. Sangeetha, "Remote sensing data-based satellite image analysis in water quality detection for public health data modelling," *Remote Sensing in Earth Systems Sciences*, vol. 7, no. 4, pp. 532–541, 2024.
- [59] J. Huang, J. Xu, Q. Chong, and Z. Li, "Black and odorous water detection of remote sensing images based on improved deep learning," *Canadian Journal of Remote Sensing*, vol. 49, no. 1, p. 2237591, 2023.
- [60] B. Wehrmann, "Solar power in Germany – output, business & perspectives — cleanenergywire.org," <https://www.cleanenergywire.org/factsheets/solar-power-germany-output-business-perspectives>, 2024, [Accessed 01-05-2025].
- [61] M. Klingler, N. Ameli, J. Rickman, and J. Schmidt, "Large-scale green grabbing for wind and solar photovoltaic development in brazil," *Nature Sustainability*, vol. 7, no. 6, pp. 747–757, 2024.
- [62] K. Bradbury, R. Saboo, T. L. Johnson, J. M. Malof, A. Devarajan, W. Zhang, L. M. Collins, and R. G. Newell, "Distributed solar photovoltaic array location and extent dataset for remote sensing object identification," *Scientific data*, vol. 3, no. 1, pp. 1–9, 2016.
- [63] Z. Xia, Y. Li, S. Guo, R. Chen, W. Zhang, P. Zhang, and P. Du, "Mapping global water-surface photovoltaics with satellite images," *Renewable and Sustainable Energy Reviews*, vol. 187, p. 113760, 2023.
- [64] Z. Yang and R. Rad, "Glosfarid: Global multispectral dataset for solar farm identification in satellite imagery," *arXiv preprint arXiv:2404.05180*, 2024.
- [65] B. Srinivasu, P. S. Rao *et al.*, "Infrastructure development and economic growth: Prospects and perspective," *Journal of business management and Social sciences research*, vol. 2, no. 1, pp. 81–91, 2013.
- [66] E. Dugoua, R. Kennedy, and J. Urpelainen, "Satellite data for the social sciences: measuring rural electrification with night-time lights," *International journal of remote sensing*, vol. 39, no. 9, pp. 2690–2701, 2018.
- [67] Z. Shah, N. Klugman, G. Cadamuro, F.-C. Hsu, C. D. Elvidge, and J. Taneja, "The electricity scene from above: Exploring power grid inconsistencies using satellite data in accra, ghana," *Applied Energy*, vol. 319, p. 119237, 2022.
- [68] Y. Ma, Y. Li, K. Feng, Y. Xia, Q. Huang, H. Zhang, C. Prieur, G. Licciardi, H. Malha, J. Chanussot *et al.*, "The outcome of the 2021 ieee grss data fusion contest-track DSE: Detection of settlements without electricity," *IEEE Journal of Selected Topics in Applied Earth Observations and Remote Sensing*, vol. 14, pp. 12 375–12 385, 2021.
- [69] E. Costa, "Industry 5.0 and SDG 9: a symbiotic dance towards sustainable transformation," *Sustainable Earth Reviews*, vol. 7, no. 1, p. 4, 2024.
- [70] J. Wu, C. O'Sullivan, F. Orlandi, D. O'Sullivan, and S. Dev, "Measurement of industrial smoke plumes from satellite images," in *IGARSS 2023-2023 IEEE International Geoscience and Remote Sensing Symposium*. IEEE, 2023, pp. 5680–5683.

- [71] Y. Sun, L. Jiang, J. Pan, S. Sheng, and L. Hao, "A satellite imagery smoke detection framework based on the mahalanobis distance for early fire identification and positioning," *International Journal of Applied Earth Observation and Geoinformation*, vol. 118, p. 103257, 2023.
- [72] C. Gómez and D. Moctezuma, "Smoke plume detection using u-net model: an application in the mexican territory," *Journal of Applied Remote Sensing*, vol. 18, no. 4, pp. 044 522–044 522, 2024.
- [73] M. Mommert, M. Sigel, M. Neuhausler, L. Scheibenreif, and D. Borth, "Characterization of industrial smoke plumes from remote sensing data," in *Tackling Climate Change with Machine Learning Workshop*, 2020, workshop paper at NeurIPS 2020. [Online]. Available: <https://www.climatechange.ai/papers/neurips2020/52>
- [74] C. Persello and M. Kuffer, "Towards uncovering socio-economic inequalities using vhr satellite images and deep learning," in *IGARSS 2020-2020 IEEE International Geoscience and Remote Sensing Symposium*. IEEE, 2020, pp. 3747–3750.
- [75] Z. Zheng, Y. Zhong, J. Wang, A. Ma, and L. Zhang, "Building damage assessment for rapid disaster response with a deep object-based semantic change detection framework: From natural disasters to man-made disasters," *Remote Sensing of Environment*, vol. 265, p. 112636, 2021.
- [76] L. Shen, Y. Lu, H. Chen, H. Wei, D. Xie, J. Yue, R. Chen, S. Lv, and B. Jiang, "S2looking: A satellite side-looking dataset for building change detection," *Remote Sensing*, vol. 13, no. 24, p. 5094, 2021.
- [77] H. Chen and Z. Shi, "A spatial-temporal attention-based method and a new dataset for remote sensing image change detection," *Remote sensing*, vol. 12, no. 10, p. 1662, 2020.
- [78] J. Li, J. Xing, S. Du, S. Du, C. Zhang, and W. Li, "Change detection of open-pit mine based on siamese multiscale network," *IEEE Geoscience and Remote Sensing Letters*, vol. 20, pp. 1–5, 2022.
- [79] S. Du, W. Li, J. Li, S. Du, C. Zhang, and Y. Sun, "Open-pit mine change detection from high resolution remote sensing images using da-unet++ and object-based approach," *International Journal of Mining, Reclamation and Environment*, vol. 36, no. 7, pp. 512–535, 2022.
- [80] Z. Xie, J. Jiang, D. Yuan, K. Li, and Z. Liu, "Gan-based sub-instance augmentation for open-pit mine change detection in remote sensing images," *IEEE Transactions on Geoscience and Remote Sensing*, vol. 62, pp. 1–19, 2023.
- [81] W. Yu, X. Zhang, R. Gloaguen, X. Xiang Zhu, and P. Ghamisi, "Minenetcd: A benchmark for global mining change detection on remote sensing imagery," *IEEE Transactions on Geoscience and Remote Sensing*, vol. 62, pp. 1–16, 2024.
- [82] A. Tsatsaris, K. Kalogeropoulos, N. Stathopoulos, P. Louka, K. Tsanakas, D. E. Tsesmelis, V. Krassanakis, G. P. Petropoulos, V. Pappas, and C. Chalkias, "Geoinformation technologies in support of environmental hazards monitoring under climate change: An extensive review," *ISPRS International Journal of Geo-Information*, vol. 10, no. 2, p. 94, 2021.
- [83] H. Singh, L.-M. Ang, and S. K. Srivastava, "Active wildfire detection via satellite imagery and machine learning: An empirical investigation of australian wildfires," *Natural Hazards*, pp. 1–24, 2025.
- [84] D. Rashkovetsky, F. Mauracher, M. Langer, and M. Schmitt, "Wildfire detection from multisensor satellite imagery using deep semantic segmentation," *IEEE Journal of Selected Topics in Applied Earth Observations and Remote Sensing*, vol. 14, pp. 7001–7016, 2021.
- [85] C. Phillips, S. Roy, K. Ankur, and R. Ramachandran, "HLS Foundation Burnscars Dataset," Aug. 2023. [Online]. Available: https://huggingface.co/ibm-nasa-geospatial/hls_burn_scars
- [86] K. Kikaki, I. Kakogeorgiou, I. Hoteit, and K. Karantzalos, "Detecting marine pollutants and sea surface features with deep learning in sentinel-2 imagery," *ISPRS Journal of Photogrammetry and Remote Sensing*, vol. 210, pp. 39–54, 2024.
- [87] M. M. Duarte and L. Azevedo, "Automatic detection and identification of floating marine debris using multi-spectral satellite imagery," *IEEE Transactions on Geoscience and Remote Sensing*, vol. 61, pp. 1–15, 2023.
- [88] K. Kikaki, I. Kakogeorgiou, I. Hoteit, and K. Karantzalos, "Detecting marine pollutants and sea surface features with deep learning in Sentinel-2 imagery," *ISPRS Journal of Photogrammetry and Remote Sensing*, 2024.
- [89] S. P. Stefanidis, N. D. Proutsos, A. D. Solomou, P. Michopoulos, A. Bourletsikas, D. Tigkas, V. Spalevic, and S. Kader, "Spatiotemporal monitoring of post-fire soil erosion rates using earth observation (eo) data and cloud computing," *Natural Hazards*, vol. 121, no. 3, pp. 2873–2894, 2025.
- [90] A. Iglseider, M. Immitzer, A. Dostálová, A. Kasper, N. Pfeifer, C. Bauerhansl, S. Schöttl, and M. Hollaus, "The potential of combining satellite and airborne remote sensing data for habitat classification and monitoring

- in forest landscapes,” *International Journal of Applied Earth Observation and Geoinformation*, vol. 117, p. 103131, 2023.
- [91] P. Potapov, S. Turubanova, M. C. Hansen, A. Tyukavina, V. Zalles, A. Khan, X.-P. Song, A. Pickens, Q. Shen, and J. Cortez, “Global maps of cropland extent and change show accelerated cropland expansion in the twenty-first century,” *Nature Food*, vol. 3, no. 1, pp. 19–28, 2022.
- [92] C. L. Crawford, R. A. Wiebe, H. Yin, V. C. Radeloff, and D. S. Wilcove, “Biodiversity consequences of cropland abandonment,” *Nature Sustainability*, vol. 7, no. 12, pp. 1596–1607, 2024.
- [93] G. I. Drakonakis, G. Tsagkatakis, K. Fotiadou, and P. Tsakalides, “Ombrianet—supervised flood mapping via convolutional neural networks using multitemporal Sentinel-1 and Sentinel-2 data fusion,” *IEEE Journal of Selected Topics in Applied Earth Observations and Remote Sensing*, vol. 15, pp. 2341–2356, 2022.
- [94] Z. Hou, Y. Qu, L. Zhang, J. Liu, F. Wang, Q. Yu, A. Zeng, Z. Chen, Y. Zhao, H. Tang *et al.*, “War city profiles drawn from satellite images,” *Nature Cities*, vol. 1, no. 5, pp. 359–369, 2024.
- [95] H. Yin, L. Eklund, D. Habash, M. B. Qumsiyeh, and J. Van Den Hoek, “Evaluating war-induced damage to agricultural land in the gaza strip since october 2023 using planetscope and skysat imagery,” *Science of Remote Sensing*, vol. 11, p. 100199, 2025.
- [96] M. Bouabid and M. Farah, “Gazadeepdav: A high resolution geotagged satellite imagery dataset for analyzing war-induced damage,” in *IGARSS 2024-2024 IEEE International Geoscience and Remote Sensing Symposium*. IEEE, 2024, pp. 8876–8879.
- [97] Y. Wang, N. A. A. Braham, Z. Xiong, C. Liu, C. M. Albrecht, and X. X. Zhu, “SSL4EO-S12: A large-scale multimodal, multitemporal dataset for self-supervised learning in Earth observation [software and data sets],” *IEEE Geoscience and Remote Sensing Magazine*, vol. 11, no. 3, pp. 98–106, 2023.
- [98] Z. Xiong, Y. Wang, F. Zhang, A. J. Stewart, J. Hanna, D. Borth, I. Papoutsis, B. L. Saux, G. Camps-Valls, and X. X. Zhu, “Neural plasticity-inspired multimodal foundation model for Earth observation,” *arXiv preprint arXiv:2403.15356*, 2024.
- [99] M. Mendieta, B. Han, X. Shi, Y. Zhu, and C. Chen, “Towards geospatial foundation models via continual pretraining,” in *Proceedings of the IEEE/CVF International Conference on Computer Vision*, 2023, pp. 16 806–16 816.
- [100] J. Jakubik, S. Roy, C. Phillips, P. Fraccaro, D. Godwin, B. Zadrozny, D. Szwarcman, C. Gomes, G. Nyirjesy, B. Edwards *et al.*, “Foundation models for generalist geospatial artificial intelligence,” *arXiv preprint arXiv:2310.18660*, 2023.
- [101] F. Liu, D. Chen, Z. Guan, X. Zhou, J. Zhu, Q. Ye, L. Fu, and J. Zhou, “RemoteCLIP: A vision language foundation model for remote sensing,” *IEEE Transactions on Geoscience and Remote Sensing*, 2024.
- [102] F. Bastani, P. Wolters, R. Gupta, J. Ferdinando, and A. Kembhavi, “Satlaspretrain: A large-scale dataset for remote sensing image understanding,” in *Proceedings of the IEEE/CVF International Conference on Computer Vision*, 2023, pp. 16 772–16 782.
- [103] G. Christie, N. Fendley, J. Wilson, and R. Mukherjee, “Functional map of the world,” in *Proceedings of the IEEE Conference on Computer Vision and Pattern Recognition*, 2018, pp. 6172–6180.
- [104] G. Sumbul, M. Charfuelan, B. Demir, and V. Markl, “BigEarthNet: A large-scale benchmark archive for remote sensing image understanding,” in *IGARSS 2019-2019 IEEE international geoscience and remote sensing symposium*. IEEE, 2019, pp. 5901–5904.
- [105] X. An, W. He, J. Zou, G. Yang, and H. Zhang, “Pretrain a remote sensing foundation model by promoting intra-instance similarity,” *IEEE Transactions on Geoscience and Remote Sensing*, vol. 62, pp. 1–15, 2024.
- [106] A. Fuller, K. Millard, and J. Green, “CROMA: Remote sensing representations with contrastive radar-optical masked autoencoders,” *Advances in Neural Information Processing Systems*, vol. 36, pp. 5506–5538, 2023.
- [107] Y. Wang, C. M. Albrecht, and X. X. Zhu, “Multi-label guided soft contrastive learning for efficient Earth observation pretraining,” *IEEE Transactions on Geoscience and Remote Sensing*, 2024.
- [108] J. Lin, F. Gao, X. Shi, J. Dong, and Q. Du, “Ss-mae: Spatial–spectral masked autoencoder for multisource remote sensing image classification,” *IEEE Transactions on Geoscience and Remote Sensing*, vol. 61, pp. 1–14, 2023.
- [109] D. Du, T. Liu, and Y. Gu, “A multimodal unified representation learning framework with masked image modeling for remote sensing images,” *IEEE Transactions on Geoscience and Remote Sensing*, vol. 62, pp. 1–16, 2024.

- [110] C. J. Reed, R. Gupta, S. Li, S. Brockman, C. Funk, B. Clipp, K. Keutzer, S. Candido, M. Uyttendaele, and T. Darrell, “Scale-mae: A scale-aware masked autoencoder for multiscale geospatial representation learning,” in *Proceedings of the IEEE/CVF International Conference on Computer Vision*, 2023, pp. 4088–4099.
- [111] D. Wang, J. Zhang, M. Xu, L. Liu, D. Wang, E. Gao, C. Han, H. Guo, B. Du, D. Tao, and L. Zhang, “Mtp: Advancing remote sensing foundation model via multitask pretraining,” *IEEE Journal of Selected Topics in Applied Earth Observations and Remote Sensing*, vol. 17, pp. 11 632–11 654, 2024.
- [112] A. Dosovitskiy, L. Beyer, A. Kolesnikov, D. Weissenborn, X. Zhai, T. Unterthiner, M. Dehghani, M. Minderer, G. Heigold, S. Gelly, J. Uszkoreit, and N. Houlsby, “An image is worth 16x16 words: Transformers for image recognition at scale,” *ICLR*, 2021.
- [113] K. He, X. Zhang, S. Ren, and J. Sun, “Deep residual learning for image recognition,” in *Proceedings of the IEEE conference on computer vision and pattern recognition*, 2016, pp. 770–778.
- [114] B. Courty, V. Schmidt, S. Luccioni, Goyal-Kamal, MarionCoutarel, B. Feld, J. Lecourt, LiamConnell, A. Saboni, Inimaz, supatomic, M. Léval, L. Blanche, A. Cruveiller, ouminasara, F. Zhao, A. Joshi, A. Bogroff, H. de Lavoreille, N. Laskaris, E. Abati, D. Blank, Z. Wang, A. Catovic, M. Alencon, M. Stechly, C. Bauer, L. O. N. de Araujo, JPW, and MinervaBooks, “Mlco2/codecarbon: v2.4.1,” May 2024. [Online]. Available: <https://doi.org/10.5281/zenodo.11171501>
- [115] United States Environmental Protection Agency, “Greenhouse gas emissions from a typical passenger vehicle,” <https://www.epa.gov/greenvehicles/greenhouse-gas-emissions-typical-passenger-vehicle>, 2018, accessed: 2025-05-21.
- [116] E. Rolf, K. Klemmer, C. Robinson, and H. Kerner, “Position: Mission critical – satellite data is a distinct modality in machine learning,” in *Forty-first International Conference on Machine Learning*, 2024. [Online]. Available: <https://openreview.net/forum?id=PQ0ERKKYJu>
- [117] C. Ren, “Geospatial foundational disappointments,” <https://christopherren.substack.com/p/geospatial-foundational-disappointments>, 2024, accessed: 2025-05-27.
- [118] N. Sardana, J. Portes, S. Doubov, and J. Frankle, “Beyond chinchilla-optimal: Accounting for inference in language model scaling laws,” in *Forty-first International Conference on Machine Learning*, 2024. [Online]. Available: <https://openreview.net/forum?id=0bmXrtTDUu>
- [119] M. Kshirsagar, C. Robinson, S. Yang, S. Gholami, I. Klyuzhin, S. Mukherjee, M. Nasir, A. Ortiz, F. Oviedo, D. Tanner *et al.*, “Becoming good at ai for good,” in *Proceedings of the 2021 AAAI/ACM Conference on AI, Ethics, and Society*, 2021, pp. 664–673.